On the Performance of Trellis Coded 8PSK with Reed Solomon codes

by
Yasuo Harada
B.E.,Keio University, 1982

A Thesis Submitted in Partial Fulfillment of the
Requirements for the Degree of

Master of Applied Science

in the Department of
Electrical and Computer Engineering

We accept this thesis as conforming
to the required standard

[redacted]
Dr. Vijay K. Bhargava (Department of ECE)

[redacted]
Dr. Qiang Wang (Department of ECE)

[redacted]
Dr. Hausi Muller (Department of Computer Science)

[redacted]
Dr. Paul Fisher (School of Health Information Science)

Supervisor: Dr. Vijay K. Bhargava

ABSTRACT

Concatenated Trellis coded 8PSK with Reed Solomon (RS) codes is studied over AWGN and Rayleigh fading channels.

Trellis coded modulation (TCM) achieves a high coding gain without any bandwidth expansion. The basic analysis of its performance is reviewed and confirmed by simulation using a truncated Viterbi decoder. Trellis coded 8PSK, which has an asymptotic coding gain of 3.6dB, can be further improved by concatenation with RS codes. By concatenating TCM with an RS code, the bandwidth of the overall system is expanded by the reciprocal of the coding rate of Reed Solomon codes. Improvement in the bit error rate performance is studied for this coding system with various combinations of RS codes.

A high rate code with R=0.9 and good bit error rate performance is chosen for further study for erasure and error decoding. Results suggest that we can improve the performance particularly at a low E_b/N_0, with sufficient reliability of decoded symbols. The reliability of the input symbols to the RS decoder is obtained by a modified Viterbi decoder. A modified Viterbi decoder is studied and the performance of the bit error rate is shown. In order to obtain an improvement in the performance, a new modified Viterbi decoder with averaged reliability information is proposed and the improvement in bit error rate is confirmed by computer simulation.

Examiners

[redacted]

Dr. Vijay K. Bhargava

[redacted]

Dr. Qiang Wang

[redacted]

Dr. Hausi Muller

[redacted]

Dr. Paul Fisher

Table of Contents

List of Figures

List of Tables

Acknowledgments

I would like to express my sincere appreciation to Professor Vijay K. Bhargava, whose guidance, support and encouragement made my study fruitful, and I would also like to express my thanks to Professor Qiang Wang who gave me valuable suggestions on my work.

My gratitude goes to the management of Matsushita Electric Industrial Co. Ltd. for giving me the chance to carry out this research as a part of their employer's training program.

Thanks also to my colleagues in the Telecommunications Laboratory at the University of Victoria, especially Ivan Fair, Rudi Carolsfeld and Gordon Webster for their help in proofreading the manuscript and suggesting improvements.

To Nobuko

Chapter 1

Introduction

Telecommunication techniques have been advancing in the area of satellite, mobile and mobile-satellite communications, leading to the realization of Personal Communication Network (PCN) and Wireless Indoor Networks in the future. A digital communication scheme which has a very high reliability on a fading channel is required, since these channels are encountered with mobile and mobile-satellite or indoor multipath conditions. With this goal, diversity techniques, forward error correcting codes, direct sequence spread spectrum and frequency hopped spread spectrum have been a focus of research at many institutions working on MSAT, GSM and cellular telephone projects. The limitation on power and bandwidth, particularly in satellite communication channels also provide motivation for research. As the required capacity of systems increases, more efficient coding techniques are needed.

Coded modulation schemes have been studied since Ungerboeck presented Trellis Coded Modulation (TCM) in 1982 [1]. In a bandwidth- and power-limited channel, TCM is a very suitable scheme because it achieves a coding gain without expansion of the bandwidth, but at the cost of complexity of the encoder and decoder. We can expect further improvement in the bit error rate performance using a concatenated coding system [4]. Since it has a high error-correcting potential, there is great interest in the performance of systems using TCM and TCM concatenated with Reed-Solomon codes.

1.1 Previous Research

The idea of a concatenated code was presented by Forney [4]. He considered three types of concatenation: source coding and outer code concatenation, outer and inner code concatenation, and inner code and modulation concatenation. His emphasis was on the inner and outer codes concatenation. In 1982 Ungerboeck introduced Trellis Coded Modulation (TCM), which falls within the category of Forney's idea of concatenation of an inner code and modulation. Ungerboeck's research stimulated intensive investigation of TCM during the 1980's. Researchers were especially interested in the performance analysis of the system in additive white Gaussian noise (AWGN) and fading channels. Divsalar and Simon [5] derived the upper bound of the error performance of TCM on a fading channel.

Concatenation of an inner code and an outer code has also been previously studied. Because of the Viterbi algorithm, interest in concatenation of convolutional codes and Reed Solomon (RS) codes has grown. A convolutional coding system can achieve a higher coding gain and improvements in the bit error performance through concatenation with an outer RS code. RS codes are often used in practice because of their high error correcting capacity, particularly for burst errors. Concatenation with RS codes is also being studied with the special interest of extracting reliability information regarding decoded symbols of the Viterbi algorithm, since with this reliability information further improvements in the system performance can be achieved.

In a manner similar to the concatenation of convolutional codes and RS codes, we can think of the concatenation of TCM and RS codes. The demodulation of TCM is based on the Viterbi decoder, so we can discuss this issue in the same way. Deng and Costello [9] reported on this concatenation system in 1989. In their paper they used the erasure and error correction scheme by applying the reliability information from the inner decoder, but their algorithm is based on an infinite decision length and it is not suitable for trun-

cated Viterbi decoders. Thus, the method by which their algorithm obtains the erasure information is not efficient for the truncated Viterbi decoders which are usually used in practice. Schaub [6] reported on the concatenated coding system of a convolutional code and an RS code using an algorithm similar to the Deng's. Hagenauer [10] was interested in the concatenated coding system of an inner convolutional code and an outer convolutional code with the Soft-Output Viterbi Algorithm (SOVA). His information on the reliability of the output symbols is given by a probability of selecting wrong path.

1.2 Significance of Research

The performance of concatenated Trellis Coded 8PSK with RS codes is investigated in this thesis. In particular, the performance of the concatenated coding system is shown with regard to the following contributions:

1. system simulation is employed to compare the simulated performance of TC-8PSK on AWGN and Rayleigh fading channels with the theoretical performance;
2. an erasure scheme is studied for RS codes;
3. performance of the concatenated coding system on AWGN channels is studied;
4. a modified Viterbi decoder is proposed for the extraction of erasure information.

1.3 Thesis Outline

The thesis consists of six chapters. This chapter, Chapter 1, has presented the background of the research and its contributions.

Chapter 2 provides an introduction to Trellis Coded Modulation. It also describes the development of the program which simulates the truncated Viterbi decoder for TCM. Simulation results are compared with the upper bound.

Chapter 3 describes Reed-Solomon codes. The characteristics of these codes are presented and then erasure and error correcting performance is studied.

In Chapter 4 we discuss concatenated TC-8PSK with various RS codes and determine the performance improvement which results from the concatenation codes of TC-8PSK and RS codes.

In Chapter 5 we discuss a modified Viterbi decoder which extracts the erasure information for RS codes. A new modified Viterbi decoder for erasure and error correction of Reed-Solomon codes is proposed. The performance improvements of a concatenated coding system of TC-8PSK and an RS code using the modified Viterbi decoder is discussed.

Finally, in Chapter 6 we conclude the thesis with a summary and suggestions for future work.

Chapter 2

Description of Trellis Coded Modulation of M-ary PSK

The basic principle of Trellis Coded Modulation was introduced by Ungerboeck in 1982 [1]. TCM is a scheme which combines modulation and coding techniques. Before TCM was introduced, modulation techniques and coding techniques were separately considered and designed. The paper by Ungerboeck shows that by considering modulation and coding as a combined technique rather than two different issues, TCM achieves higher coding gain without bandwidth expansion.

This chapter provides an introductory description of Trellis Coded 8-ary PSK.

2.1 M-ary PSK

In this section we describe MPSK signals over an additive white Gaussian channel. MPSK is chosen because these modulation schemes have the constant envelope characteristics which are especially favorable for digital satellite communications. We shall show the bandwidth efficiency of MPSK and its performance over a noisy channel. MPSK signals can be written as:

$$S_i(t) = \sqrt{\frac{2E_s}{T_s}} \cos\left(\omega_0 t - \frac{2\pi}{M} i\right) \qquad \begin{matrix} 0 \le t \le T_s \\ i = 1, \ldots, M, \end{matrix} \tag{2.1}$$

where E_s is the energy per symbol, T_s is the symbol duration and ω_0 is the carrier frequency. The signal is detected in orthonormal space using the following two axes:

$$\psi_1 = \sqrt{\frac{2}{T_s}}\cos\omega_0 t$$
$$\psi_2 = \sqrt{\frac{2}{T_s}}\sin\omega_0 t \tag{2.2}$$

where the amplitude $\sqrt{2/T_s}$ is chosen to normalize the expected output of the integrators Z_1, Z_2 as shown in Figure 2.1. Figure 2.1 shows the correlator receiver for MPSK signals. The detection performance of this receiver is equivalent to that of a matched filter detector.

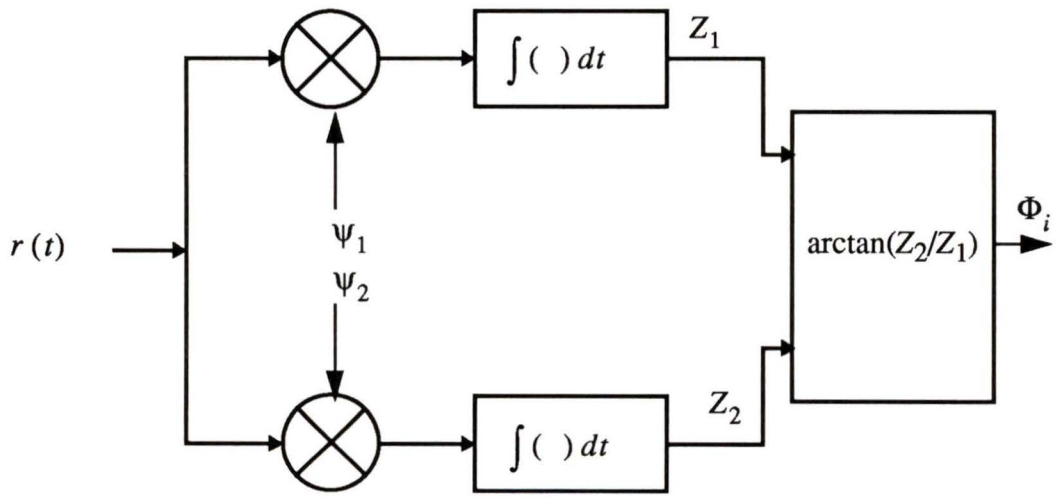

Figure 2.1 The correlator for MPSK using orthonormal basis functions

The received signal is written as the sum of the noise and the desired signal:

$$r(t) = \sqrt{\frac{2Es}{T_s}} \cos(\omega_0 t - 2\frac{\pi}{M} i) + n(t)$$

$$= \sqrt{\frac{2E_s}{T_s}} (\cos(\frac{2\pi i}{M}) \cos\omega_0 t + \sin(\frac{2\pi i}{M}) \sin\omega_0 t) + n(t), \tag{2.3}$$

where $n(t)$ is the additive white Gaussian noise component with two-sided spectral density $N_0/2$. For the case of M=8, the signal constellation may be depicted as in Figure 2.2.

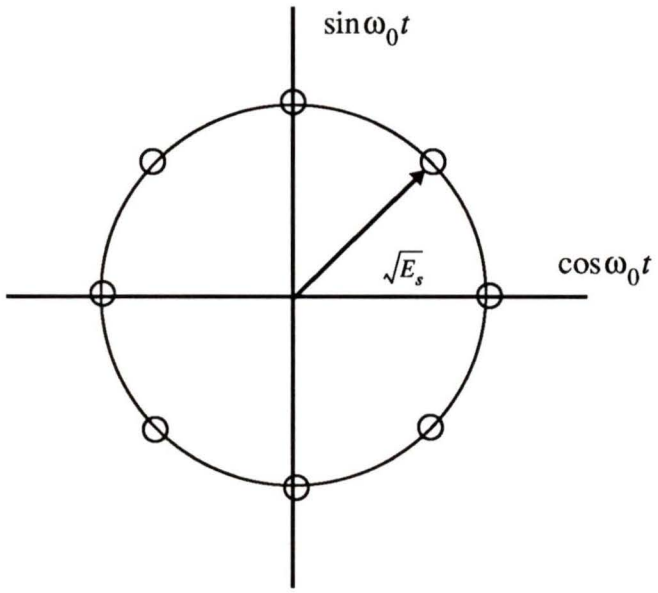

Figure 2.2 The constellation of an 8-ary PSK signal

The output of the correlator of ψ_1 axis can be written as:

$$
\begin{aligned}
Z_1 &= \int r(t)\,\psi_1 dt \\
&= \int_0^{T_s} \left(\sqrt{E_s}\cos\left(\frac{2\pi i}{M}\right)\sqrt{\frac{2}{T_s}}\cos\omega_0 t + \sqrt{E_s}\sin\left(\frac{2\pi i}{M}\right)\sqrt{\frac{2}{T_s}}\sin\omega_0 t \right) \bullet \psi_1 dt \\
&\quad + \int_0^{T_s} n(t)\,\psi_1 dt
\end{aligned}
\tag{2.4}
$$

As defined in Equation (2.2), ψ_1 and ψ_2 are the orthonormal bases (i.e., $\int_0^{T_s} \psi_i \cdot \psi_j dt = 1$ if $i = j$, otherwise $\int_0^{T_s} \psi_1 \cdot \psi_2 dt = 0$). Thus we can derive the output of the correlator as in the following equations.

$$
\begin{aligned}
Z_1 &= \sqrt{E_s} + \int n(t)\,\psi_1 dt \\
Z_2 &= \sqrt{E_s} + \int n(t)\,\psi_2 dt
\end{aligned}
\tag{2.5}
$$

The integrand is called narrow band noise: $\int n(t)\psi_1 dt = \frac{N_0}{2}$, where N_0 is the one-sided power spectral density of the white Gaussian noise.

The decision at the output is made using the phase information, which is performed by the phase decision function followed by the coherent detector shown in Figure 2.1. The phase is decided by $\Phi_i = \arctan(Z_1/Z_2)$. The decision rule is that $\hat{S}_i(t)$ is transmitted when $\left(\frac{2\pi}{M}i - \frac{\pi}{M}\right) \le \Phi_i \le \left(\frac{2\pi}{M}i + \frac{\pi}{M}\right)$. Since $n(t)$ is white Gaussian noise, the probability of symbol error Pe is given by the following equation [29]:

$$
Pe(M) \approx 2Q\left(\sqrt{\frac{2E_s}{N_0}}\sin\frac{\pi}{M}\right) \tag{2.6}
$$

Now the probability of bit error is obtained by using the relation between the symbol error rate Pe and the bit error rate Pb. For M-ary PSK, we can approximate $Pb = \frac{Pe}{\log_2 M}$ [28] for the case of Gray-coding. Figure 2.3 shows the bit error rate performance for M-ary PSK.

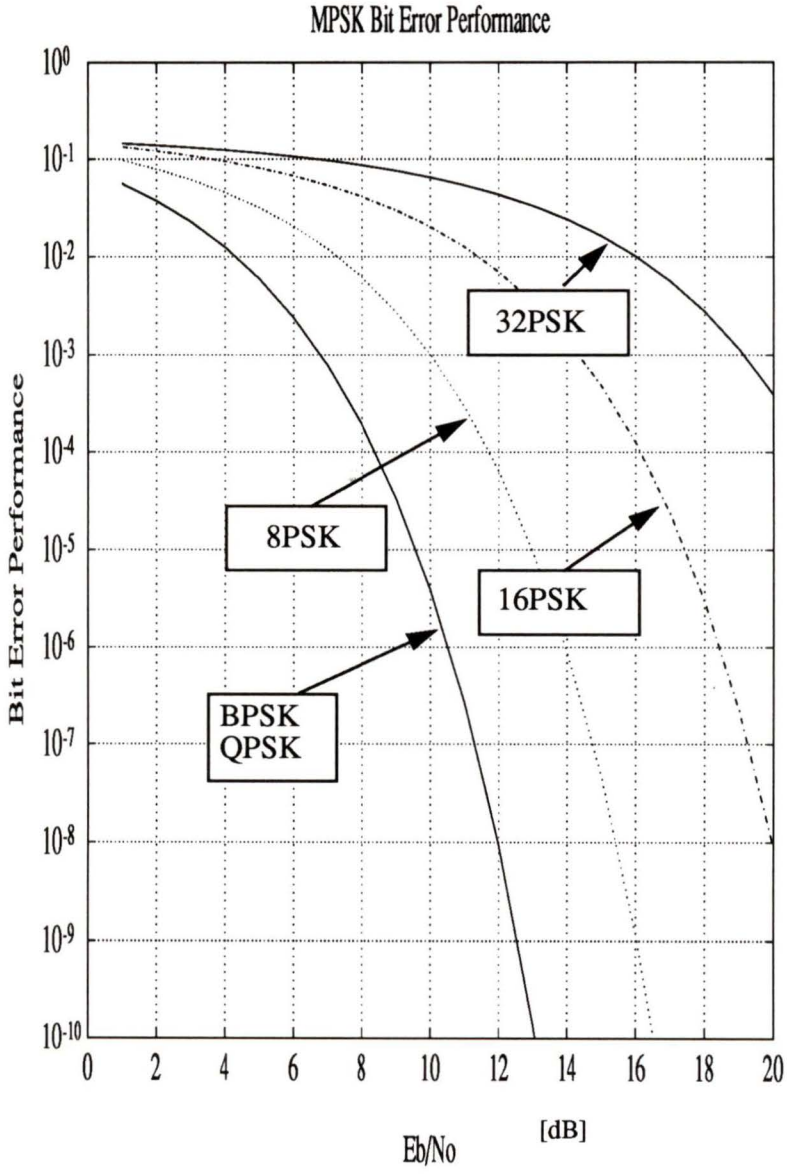

Figure 2.3 The bit error performance of M-ary PSK on an AWGN channel

2.2 Trellis Coded Modulation

A convolutional code can be represented by either a finite state machine model or the trellis diagram. In this thesis we use 8PSK to investigate the performance of Trellis Coded Modulation. TC-8PSK with 8 states is discussed here. The 8-state trellis coded modulation may be considered to require comparatively less decoder complexity when we take its coding gain into consideration, and the bandwidth efficiency is as good as that of 4PSK. When we transmit symbols by 8PSK instead of 4PSK within a given bandwidth, the data rate becomes 3/2, because uncoded 8PSK's bandwidth efficiency is 3 bits/s/Hz while for 2PSK it is 2bits/s/Hz. If we choose a rate 2/3 convolutional code to generate the symbols for 8PSK, we achieve the same overall bandwidth efficiency in terms of information.

The bit error rate performance can be improved by using TCM. The improvement in E_b/N_0 is roughly discussed by the asymptotic coding gain, which is calculated by the Euclidean distance between the correct path and the most likely incorrect path. For the case of 8 state TC-8PSK, the coding gain is 3.6 dB. This coding gain is sometimes enough for the additive white Gaussian noise channel, which is the channel model for satellite communications with fixed receiver sites. In the case of mobile satellite communication, a greater system margin is required because of signal fading.

2.2.1 TC-8PSK Encoder

The TC-8PSK encoder is shown in Figure 2.4.

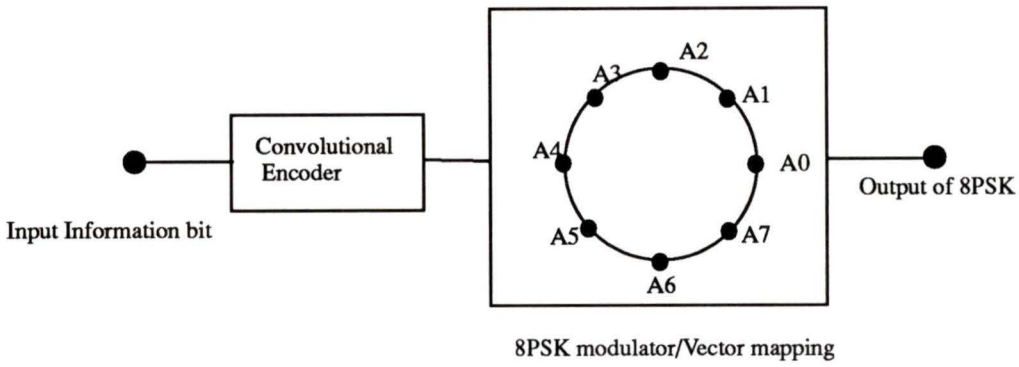

Figure 2.4 TC-8PSK Encoder

The input information bits are fed into the $(n,k,m)=(3,2,3)$ convolutional encoder, where n is the number of output bits from the encoder, k is the number of input bits, and m is the number of registers. In this case the code rate is 2/3 and the 3 output bits are fed into the 8PSK modulator. The mapping or assignment of the output symbols of a convolutional encoder to possible phases of 8PSK signal is done by natural code mapping (Table 2.1). Gray code mapping [25] is often used in conventional PSK modulation techniques. However, in the case of TCM it doesn't have the same effect as conventional PSK since the Viterbi decoder is designed for the path metric rather than the Euclidean distance between the symbols in its signal constellation.

A schematic diagram of the (3,2,3) convolutional encoder used in the research for this thesis is shown in Figure 2.5.

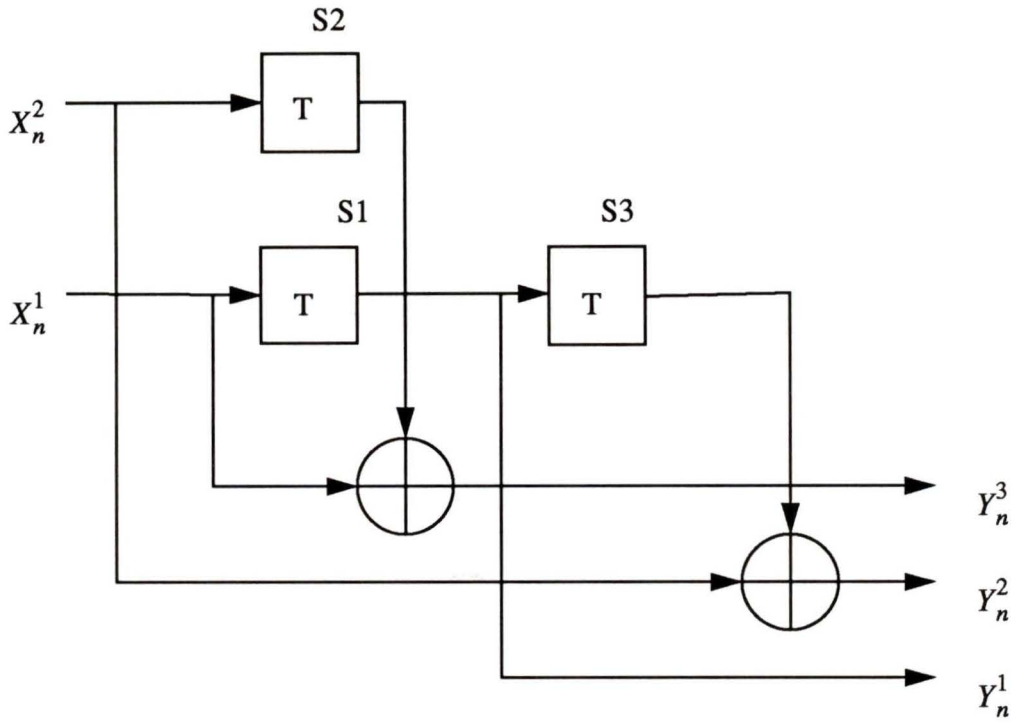

Figure 2.5 8-State convolutional encoder for TC-8PSK

The input symbol at $t=nT_s$ is comprised of two bits (X_n^1, X_n^2) which are fed into the encoder during a symbol interval, giving the output of the encoder (Y_n^1, Y_n^2, Y_n^3). The three registers realize the convolutional operation for this encoder with Exclusive OR adders. The contents of the registers are labeled S1,S2,S3, a set of the contents (S1,S2,S3)

is called a state of the convolutional encoder. At the initial stage, all registers are set to zero. The output of the decoder can be obtained by the following equation, which shows the connections in Figure 2.5:

$$\begin{aligned} Y_n^1 &= X_{n-1}^1 \\ Y_n^2 &= X_{n-2}^1 + X_n^2 \\ Y_n^3 &= X_n^1 + X_{n-1}^2 \end{aligned} \tag{2.7}$$

The phase of the output signal of the 8 PSK modulator is determined by the $Y^j{}_n$ as in Table 2.1.

$Y^3{}_n, Y^2{}_n, Y^1{}_n$	signal vector	phase
0 0 0	A0	0
0 0 1	A1	$\pi/4$
0 1 0	A2	$2\pi/4$
0 1 1	A3	$3\pi/4$
1 0 0	A4	π
1 0 1	A5	$5\pi/4$
1 1 0	A6	$6\pi/4$
1 1 1	A7	$7\pi/4$

Table 2.1. 8 PSK mapping

The 8PSK signal mapping follows a natural code mapping of $\boldsymbol{Y}_\mathbf{n}$ to Aj, j=0,...7, which are the labels representing each of the vector components in Figure 2.4. Equation (2.1) may also be applied to represent these vectors.

We can construct the trellis diagram for 8state TC-8PSK as shown in Figure 2.6.

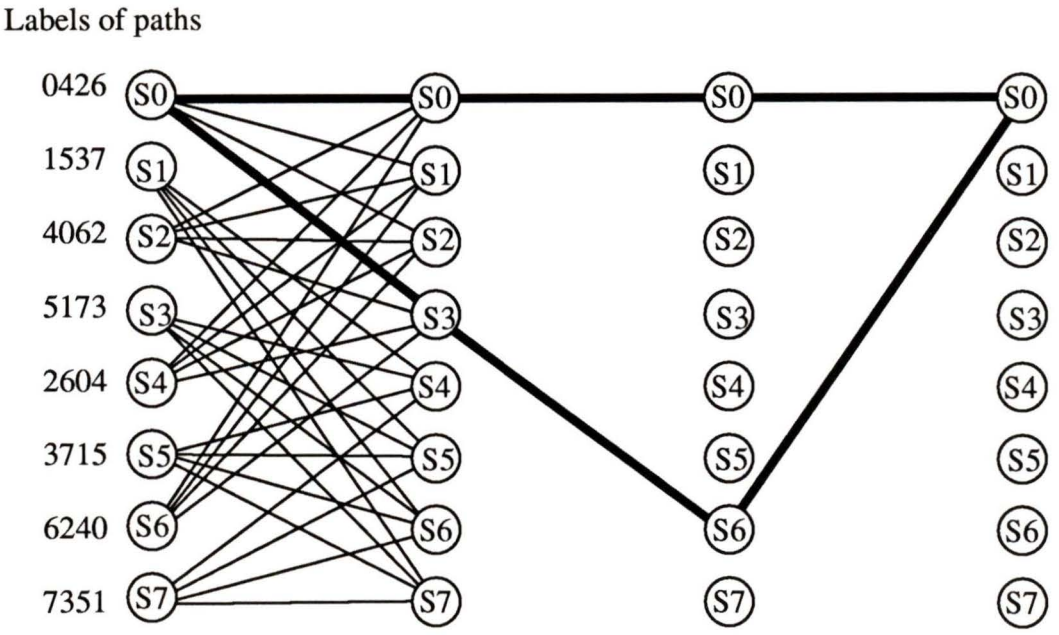

Figure 2.6 Trellis diagram for eight-state TC-8PSK

The trellis diagram shows the transition paths between states for each interval. Each branch should have the output vector labelled as A0 to A7. In Figure 2.6 for simplicity, we write only the number without the letter A and put all four digits associated with the branch vector labels next to the state number Sj. The first digit in group of four is associated with the uppermost transition branch from a state to state in the next interval. The next digit in each group is for the second highest transition branch and so on. In order to understand the state transition we redraw the transition diagram for the state S0. Each state has four possible branches associated with the two bit inputs (X_n^2, X_n^1), as shown in Figure 2.7.

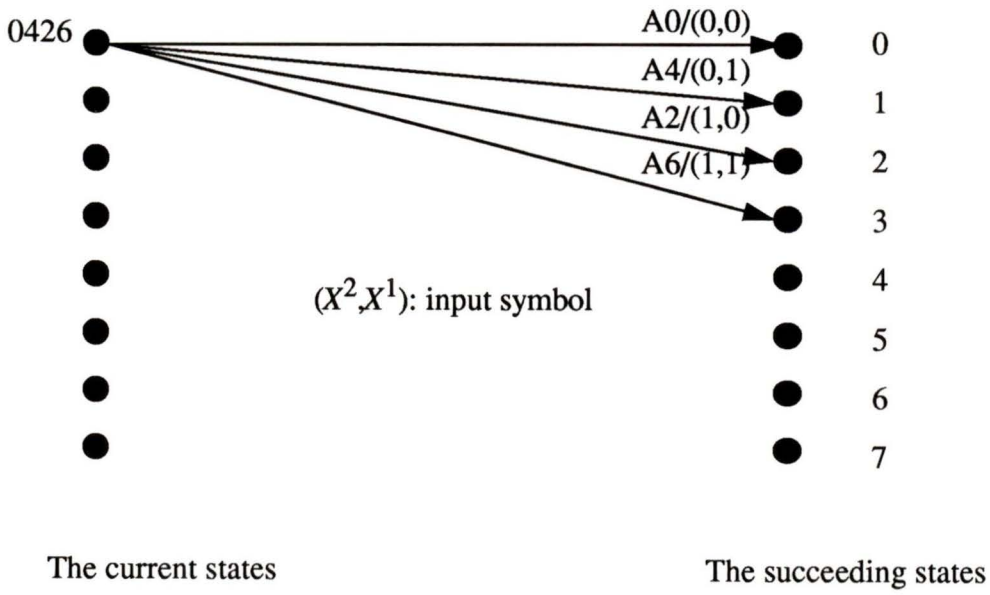

Figure 2.7 State transition

The paths marked by the solid bold lines in Figure 2.6 give the free distance, d_{free}, which gives the asymptotic coding gain. d_{free} is defined as follows. Among all possible paths, we choose pairs of paths merging in a given state from a common original state. We can choose one pair of paths, which has the smallest difference in their path metrics, i.e. the cumulative Euclidean distance of paths among all possible combinations. This distance between the two paths is defined as d_{free}. When E_b/N_0 is relatively high, we can say the coding gain is the ratio of the square of the free distance d_{free}^2 and the minimum Euclidean distance d_{min}^2 of 2^m-ary PSK signals. In the case of TC-8PSK, m is 2. This is called asymptotic coding gain. The asymptotic coding gain γ is calculated for the case of the event shown in Figure 2.6 as follows:

$$\gamma = 10 \cdot \log \frac{d_{free}^2}{d_{min}^2} = 10 \cdot \log \frac{((A0 - A6)^2 + (A0 - A7)^2 + (A0 - A6)^2)}{2} \qquad (2.8)$$

2.2.2 Performance of the Bit Error Rate

Two important measures of system performance are asymptotic coding gain, which was discussed in the previous section, and the upper bound of the bit error rate. The asymptotic coding gain is the limiting value of the coding gain at high E_b/N_0. This criterion is therefore not appropriate for designing communication systems when E_b/N_0 is low. An alternative is to use the upper bound on the bit error rate performance. In this section, we derive the upper bound of the bit error performance of TC-8PSK. Figure 2.8 shows the system model.

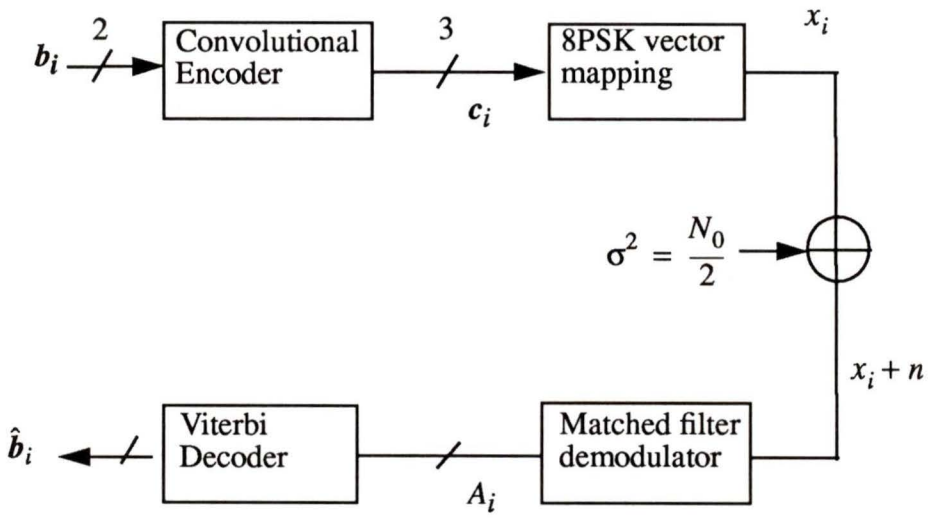

Figure 2.8 TCM system model

In Figure 2.8, $\boldsymbol{b}_i$ is the input symbol at $t = T_s i$, where T_s is the symbol period, and $\boldsymbol{c}_i$ is the output symbol of the *m/m*+1 convolutional encoder. In the case of rate 2/3 TC-8PSK, $\boldsymbol{b}_i$ is 2 bits (b_i^1, b_i^0) and the output of the convolutional encoder is 3 bits (c_i^2, c_i^1, c_i^0). The vector $\boldsymbol{c}_i$ is mapped into x_i with the mapping function of $f(\boldsymbol{c}_i)$. This function is equivalent to Table 2.1.

In order to obtain the error event probability we observe the signal sequence with a length of L as follows:

$$\overline{B}_L = (b_0, b_1, \ldots, b_{L-1}) \tag{2.9}$$

$$\overline{C}_L = (c_0, c_1, \ldots, c_{L-1}) \tag{2.10}$$

$$\overline{X_L} = f(C_L) \tag{2.11}$$

Since the function f is linear and $\boldsymbol{c}_i$ and x_i have a one-to-one correspondence, we can write C_L instead of X_L for the notation. The pairwise error probability $P[\overline{X_L} \rightarrow \overline{X'_L}]$ is the probability that the output sequence X_L' is incorrectly chosen when the transmitted signal is X_L.

Taking the averages of all possible sequences of X_L, we can obtain the probability of error events by the form of union bound [30] as:

$$P(e) \leq \sum_{L=1}^{\infty} \sum_{\overline{X_L}} P[\overline{X_L}] \sum_{\overline{X'_L} \neq \overline{X_L}} P[\overline{X_L} \rightarrow \overline{X'_L}] \tag{2.12}$$

Since X_L and C_L have a one-to-one correspondence, we can rewrite the above equation by using notation C_L which is the label of the trellis as the output of a convolutional

encoder.

The Bhattacharyya [27] bound gives the pairwise events error,

$$P[\overline{C}_L \rightarrow \overline{C}'_L] \leq exp\{-\frac{E_s}{4N_0}\left\|f(\overline{C_L}) - f(\overline{C'_L})\right\|^2\}$$

$$= exp\left\{-\frac{E_s}{4N_0}\sum_{n=1}^{L}\left\|f(c_n) - f(c'_n)\right\|^2\right\}. \tag{2.13}$$

We define the $W(E_L)$ function as follows

$$W(E_L) = \sum_{C_L} P[C_L] Z^{\left\|f(\overline{C_L}) - f(\overline{C_L} + \overline{E_L})\right\|^2} \tag{2.14}$$

where $Z=exp(-Es/4N_0)$ and E_L is the error sequence. Then using an error sequence, we can write the $P(e)$ as follows

$$P(e) = \sum_{L=1}^{\infty}\sum_{E_L \neq 0} W(E_L). \tag{2.15}$$

Recall that the transfer function of the state transition $T(D)$ contains all possible cases as the power series of D, where the exponent of D indicates the metric difference which an erroneous transition generates. Therefore, when D is replaced by Z, we can write $P(e)$ in terms of $T(D)$ as follows [30]

$$P(e) \leq T(D)\Big|_{D = exp(-\frac{Es}{4N0})}. \tag{2.16}$$

In order to get the pairwise error event probability we can calculate the transfer function of $D=Z$. By using the error state diagram we can calculate $T(D)$ as the sum of the error weight profile [30] which is defined as:

$$W(\bar{e}) = \frac{1}{2^m} \sum_{\bar{C}_{c1=0}} D^{\| f(\bar{C}_{c1=0}) - f(\bar{C}_{c1=0} + \bar{e}) \|^2} \tag{2.17}$$

Now, in the case of rate 2/3 TC-8PSK, m is 2 and we can calculate the error weight profiles of each of the error vectors $e=(e3,e2,e1)$ for $c=(c3,c2,0)$ as follows.

$$W(000) = 1 \tag{2.18}$$

$$\begin{aligned} W(001) &= \frac{1}{4} \{ D^{\| f(000) - f(001) \|^2} + D^{\| f(010) - f(011) \|^2} \\ &\quad + D^{\| f(100) - f(101) \|^2} + D^{\| f(110) - f(111) \|^2} \} \\ &= D^{0.5858} \end{aligned} \tag{2.19}$$

In the same manner we can determine all the error weight profiles shown in Table 2.2.

w(n)	W(e3,e2,e1)	Error profiles
w(0)	W(0,0,0)	D^0
w(1)	W(0,0,1)	D^0.5858
w(2)	W(0,1,0)	D^2.0
w(3)	W(0,1,1)	(D^0.5858+D^3.1414)/2
w(4)	W(1,0,0)	D^4
w(5)	W(1,0,1)	D^3.1414
w(6)	W(1,1,0)	D^2
w(7)	W(0,1,1)	(D^0.5858+D^3.1414)/2

Table 2.2. Error Weight Profiles

The bit error rate is obtained from the next equation [30]:

$$Pb = \frac{1}{m}\frac{\partial}{\partial I}T(D,I)\,|_{I=1,\,D=exp(-Es/4N0)} \tag{2.20}$$

where I is the non-determinate parameter and its power indicates the number of bit errors which occur in each transition. $T(D,I)$ is obtained by

$$T(D,I) = \sum_{e} I^{n} W(e) \tag{2.21}$$

where the power n of I is the squared Euclidean distance of the error vector e.

The error state diagram is shown in Figure 2.9. Each transition branch is labelled by its error weight profiles which are also given in Table 2.3.

Branch	Label	Branch	Label
α1	$IW(4)$	α16	$W(2)$
α2	$IW(2)$	α17	$IW(6)$
α3	$I^2W(6)$	α18	$IW(0)$
α4	$W(4)$	α19	$I^2W(4)$
α5	$IW(0)$	α20	$W(3)$
α6	$IW(6)$	α21	$IW(7)$
α7	$I^2W(2)$	α22	$IW(1)$
α8	$W(1)$	α23	$I^2W(5)$
α9	$IW(5)$	α24	$W(6)$
α10	$IW(3)$	α25	$IW(2)$
α11	$I^2W(7)$	α26	$IW(4)$
α12	$W(5)$	α27	$I^2W(0)$
α13	$IW(1)$	α28	$W(7)$
α14	$IW(7)$	α29	$IW(3)$
α15	$I^2W(3)$	α30	$IW(5)$
		α31	$I^2W(1)$

Table 2.3. Branch labels of an error state diagram

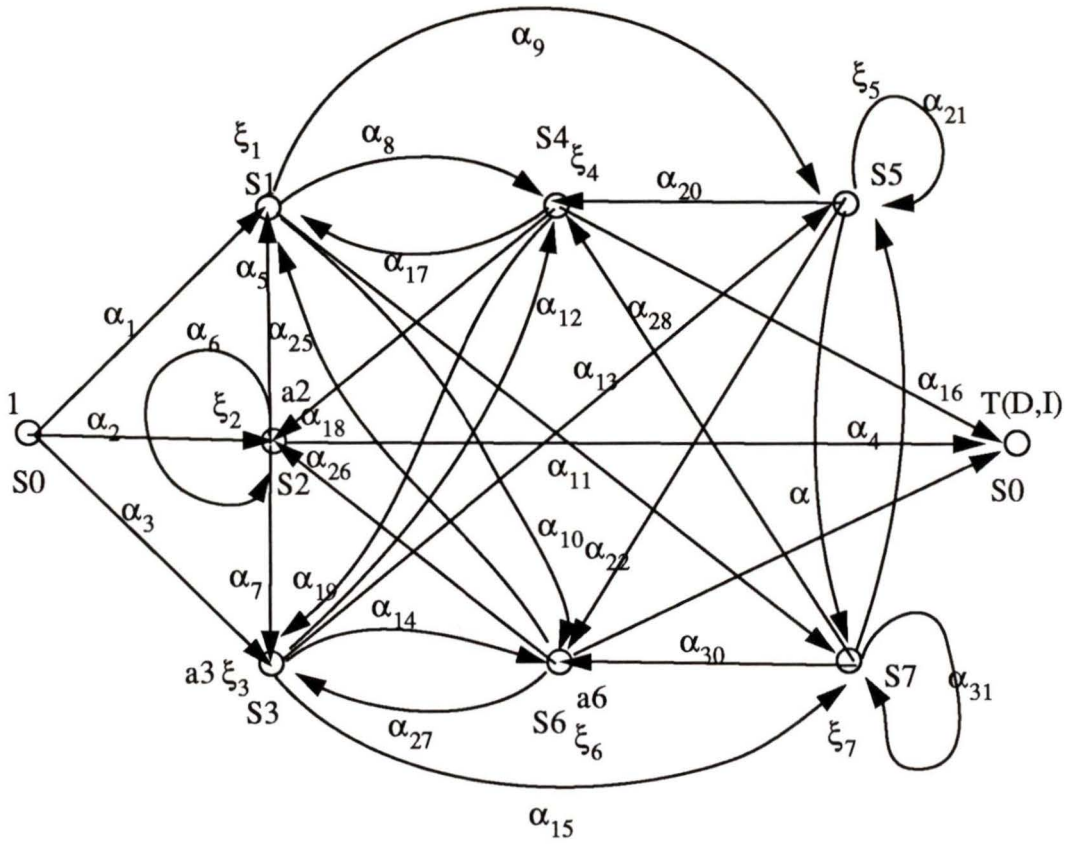

Figure 2.9 State transition diagram for 8 state Trellis

From the branch and the state diagrams we can derive the equation,

$$T(D,I) = \alpha_4\xi_2 + \alpha_{16}\xi_4 + \alpha_{24}\xi_6 \tag{2.22}$$

where

$$\begin{bmatrix}\xi_1\\ \xi_2\\ \xi_3\\ \xi_4\\ \xi_5\\ \xi_6\\ \xi_7\end{bmatrix} = \begin{bmatrix} 1 & -\alpha_5 & 0 & -\alpha_{17} & 0 & -\alpha_{25} & 0\\ 0 & 1-\alpha_6 & 0 & -\alpha_{18} & 0 & -\alpha_{26} & 0\\ 0 & -\alpha_7 & 1 & -\alpha_{19} & 0 & -\alpha_{27} & 0\\ -\alpha_8 & 0 & -\alpha_{12} & 1 & -\alpha_{20} & 0 & -\alpha_{28}\\ -\alpha_9 & 0 & -\alpha_{13} & 0 & 1-\alpha_{21} & 0 & -\alpha_{29}\\ -\alpha_{10} & 0 & -\alpha_{14} & 0 & -\alpha_{22} & 1 & -\alpha_{30}\\ -\alpha_{11} & 0 & -\alpha_{15} & 0 & -\alpha_{23} & 0 & 1-\alpha_{31}\end{bmatrix}^{-1} \begin{bmatrix}\alpha_1\\ \alpha_2\\ \alpha_3\\ 0\\ 0\\ 0\\ 0\end{bmatrix} \tag{2.23}$$

Equation (2.22) can be evaluated by computers; the first derivative of $T(D,I)$ in terms of I gives the bit error rate according to the Equation (2.20).

Figure 2.10 shows the performance of the TC-8PSK with 8 states. The upper bound of TCM is plotted using Equation (2.20). The simulation result is also shown. Figure 2.11 shows the results in case of a Rayleigh fading channel. For a fading channel we can use the same Equation (2.20) by replacing each of error weight profiles by the mean of the Rayleigh distribution random variable.

Simulation was done using the program discussed in the next section.

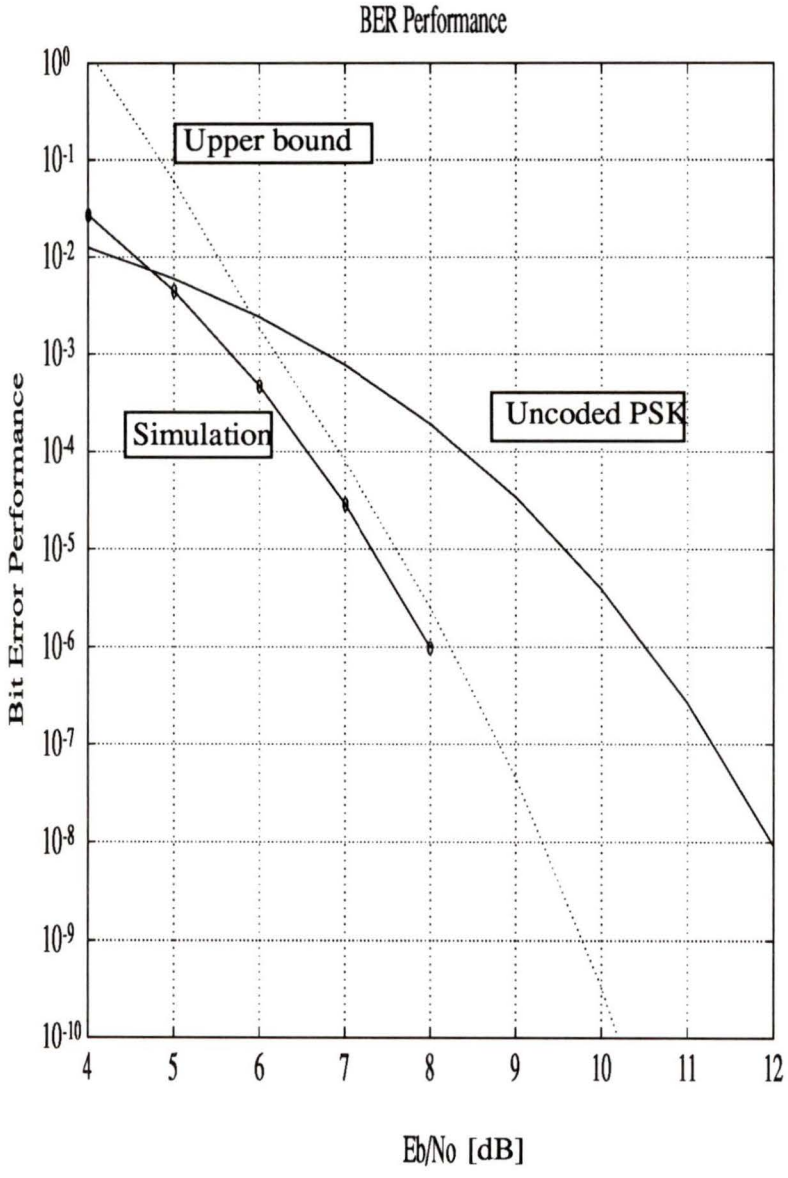

Figure 2.10 The performance of TC-8PSK with 8 states

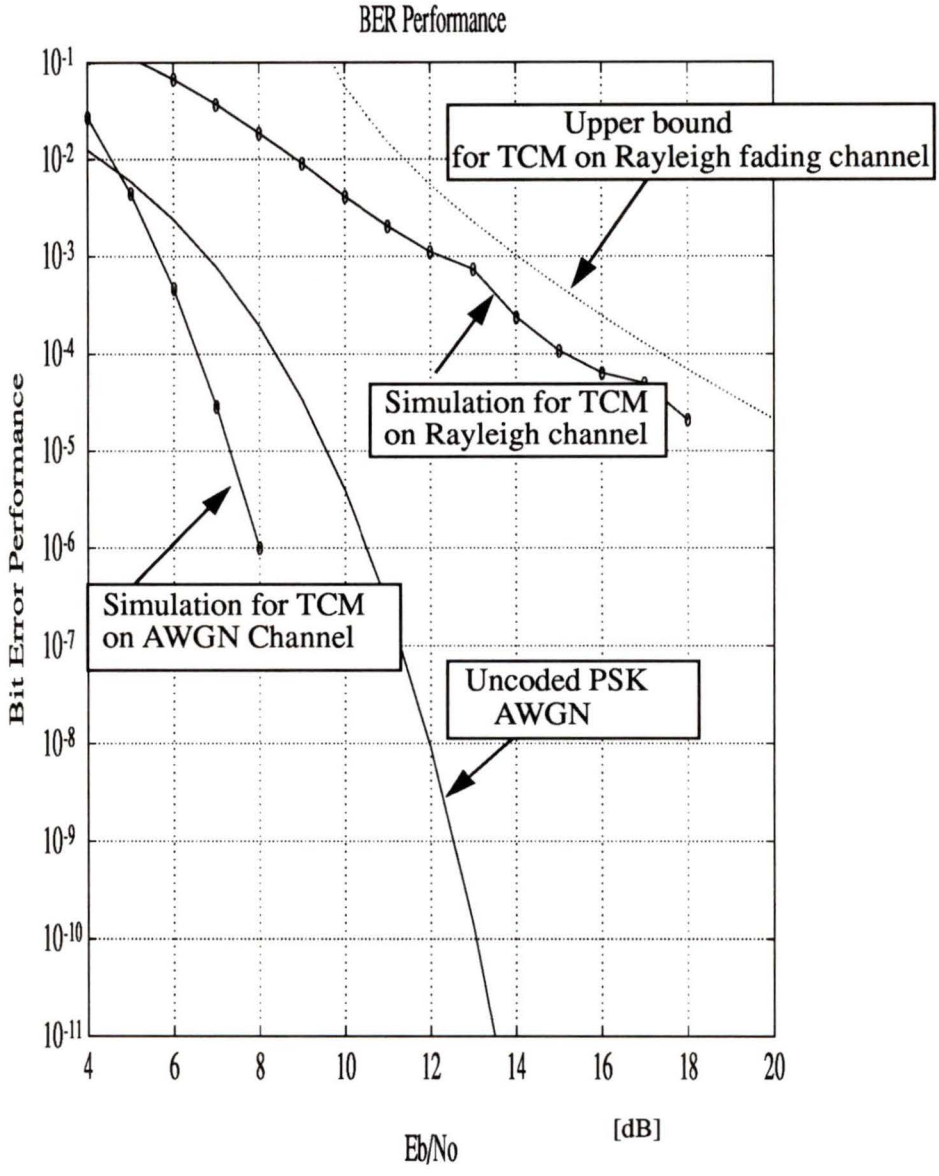

Figure 2.11 The performance of TC-8PSK on Rayleigh fading channel

2.2.3 Viterbi Decoder

The Viterbi decoder is well known as the maximum likelihood decoder for convolutional codes. TCM is also decoded using a Viterbi decoder, since the encoder uses a convolutional code which can be represented by a trellis diagram.

Figure 2.12 shows a model of a communication system. The encoded symbols c_i determine the 8PSK vectors, and white Gaussian noise is added on the channel. The demodulator is realized by a matched filter as shown before. The filter output can be written as

$$y_i = \sqrt{E_s} exp\,(-j\phi_i) + n_i. \tag{2.24}$$

At each symbol time, the output of the matched filter is fed into a Viterbi decoder.

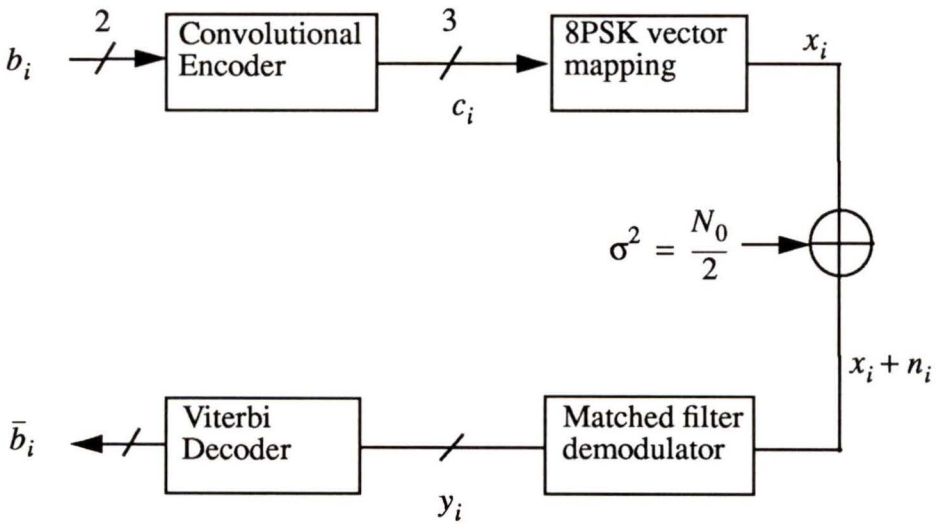

Figure 2.12 Super-channel for concatenated coding system

The Viterbi algorithm uses the trellis diagram for decoding. We will therefore review the basic concept of a truncated Viterbi decoder. We have an L-stage window to observe the trellis diagram at the decoder. Observing L stages, we will decode the symbol b_i, which means that the symbol b_i at $t=iT_s$ is decoded by the input sequence $\{y_i,y_{i+1},\ldots,y_{i+L}\}$ with a delay of LT_s. The task for the decoder is to choose the most likely path among possible transition paths in the window. The path metric is

$$M(\boldsymbol{y}, \boldsymbol{x}) = \sum_{n=1}^{L} |y_n - \rho x_n|^2 \tag{2.25}$$

where y_n is the input component of the Viterbi decoder and x_n is the transmitted vector. The received signal amplitude is a random variable denoted by ρ in case of a Rayleigh fading channel. It is assumed that we have perfect channel side information. The most likely path is the path with the minimum cumulative path metric.

Each symbol received is input into the Viterbi decoder. We shift the observation window 1 stage and obtain the path with the minimum path metric. The first symbol, which is the label of this path in its trellis diagram, is decoded as the transmitted symbol.

Figure 2.13 shows an example of the trellis diagram of the decoder. The lines indicate the decoded path with the minimum path metric 0. The number shows the number of the previous state to which the current state must be connected for the cumulative path metrics to be minimized. The window length is chosen to be 15-stage, which is 5 times

the constraint length.

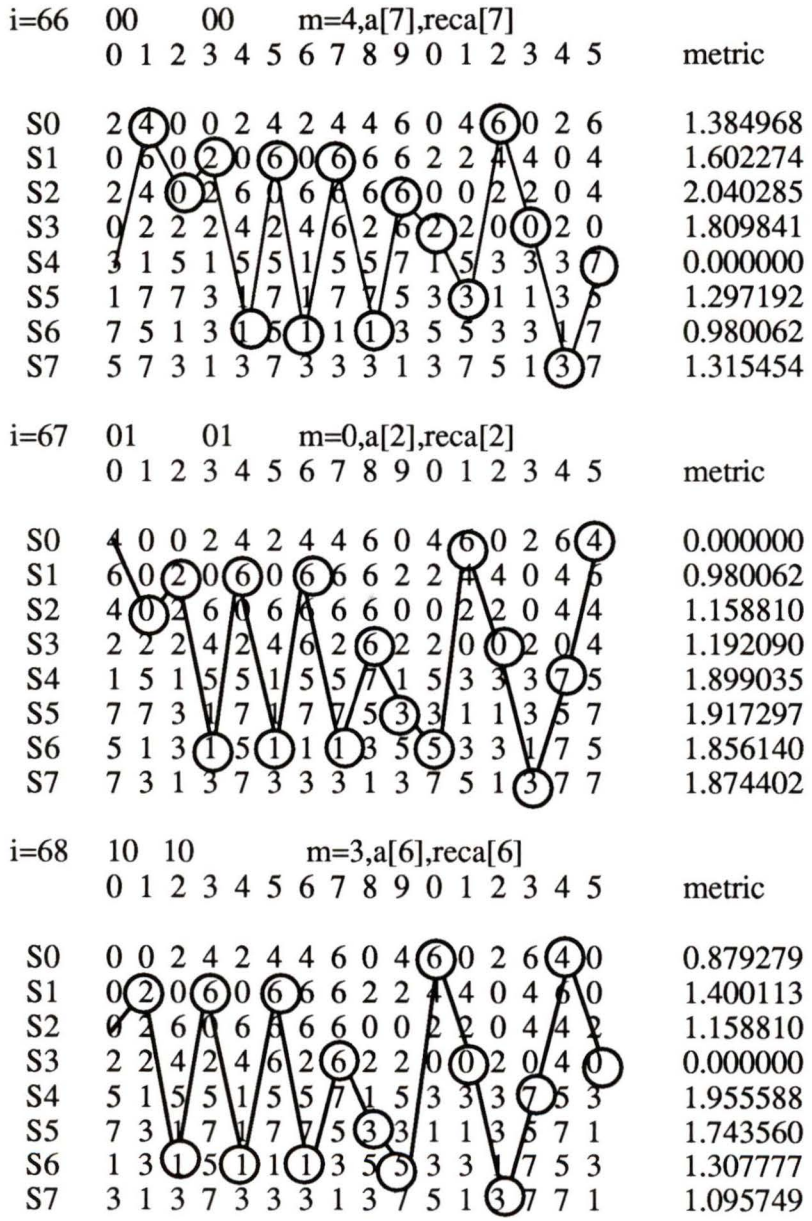

Figure 2.13 Trace back of a trellis diagram

Figure 2.14 shows the flow-chart of the truncated Viterbi decoder which is programmed for the simulation.

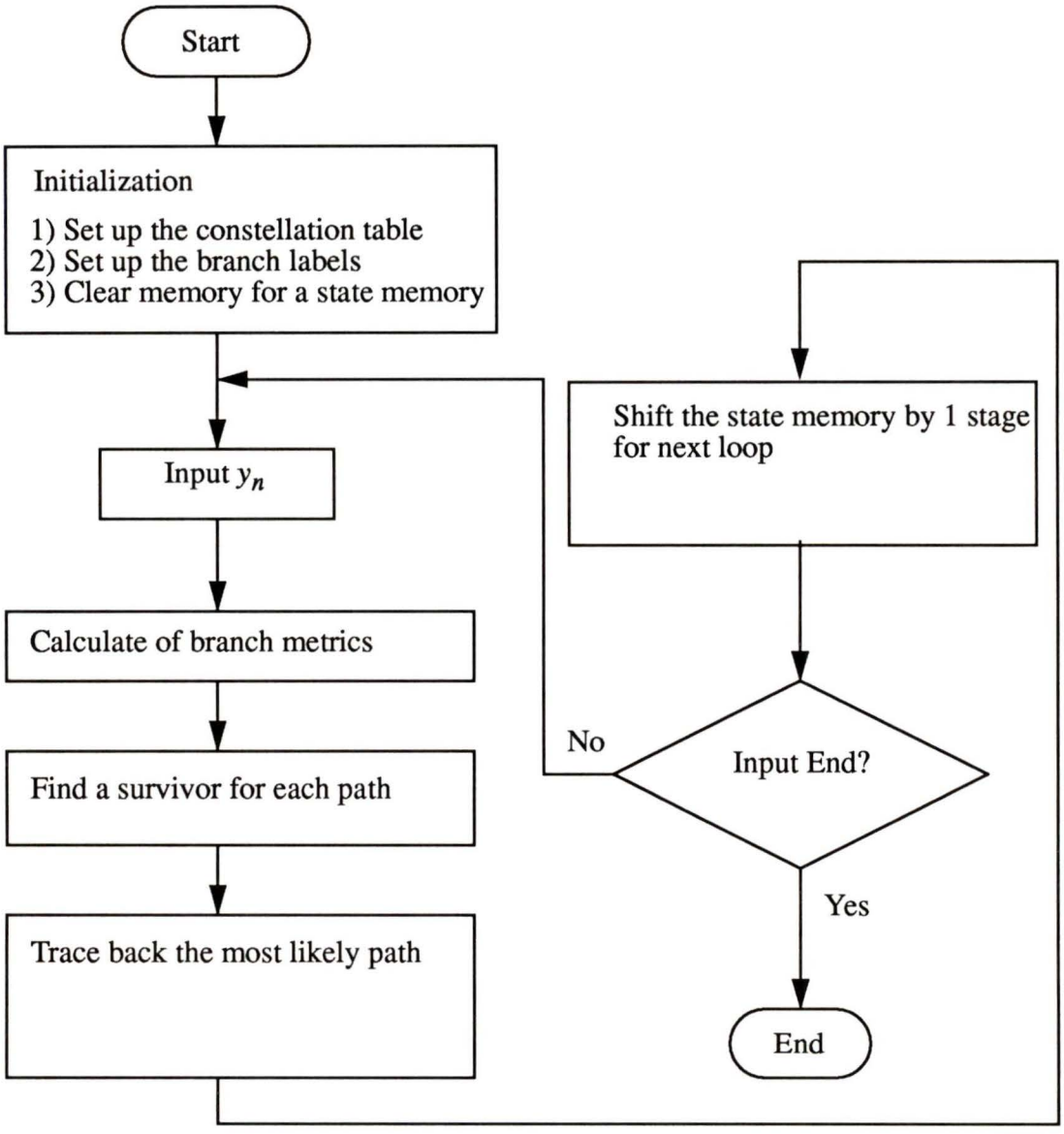

Figure 2.14 The flow chart of the truncated Viterbi decoder

2.3 Summary

In this chapter M-ary PSK and its trellis coded modulation was presented. The performance of TC-8PSK was determined by the upper bound and through simulation of the truncated Viterbi decoder. The analysis considered transmission over the AWGN channel and the Rayleigh fading channel. The results agree well with the literature [8]. This confirms that the simulation is appropriate for comparing the performance of TCM in later chapters.

Chapter 3

Reed Solomon Codes

3.1 Description of Codes

A Reed-Solomon code (RS code) is an important sub-class of BCH codes. A t-error correcting Reed-Solomon code with symbols from GF(q=2^m) is defined by the following parameters:

Block length:	$n=q-1$
Number of parity-check digits:	$n-k=2t$
Minimum distance:	$d_{min} = 2t+1.$

In other words, the number of bits of a symbol is q, and the number of symbols in a code word is one less than the number of bits per symbol. The number of parity check symbols is exactly twice the number of correctable symbols. The minimum distance between code words is exactly $2t + 1$. Let α be a primitive element of GF(2^m). The generator polynomial of a primitive t-error-correcting Reed-Solomon code of length $2^m - 1$ is

$$g(X) = (X+\alpha)(X+\alpha^2)\ldots(X+\alpha^{2t}) \tag{3.1}$$

RS codes are said to be maximum distance separable because the minimum distance is given by $n-k+1$, which is equal to the upper bound of the Hamming distance.

3.2 Decoding RS Codes

RS codes are nonbinary, so decoding requires that both the location of errors and the magnitude of the errors be calculated. We will study the decoder developed by Peterson [24] to understand the RS codes. Suppose that an RS code is constructed based on the field element α. Then the error polynomial is

$$e(x) = e_{n-1}x^{n-1} + e_{n-2}x^{n-2} + \ldots + e_1 x + e_0 \tag{3.2}$$

where at most t coefficients are non-zero. Suppose that ν errors actually occur, $0 \leq \nu \leq t$, and that they occur at the unknown locations $i_1, i_2, \ldots, i_\nu$. The error polynomial can be written as:

$$e(x) = e_{i1}x^{i1} + e_{i2}x^{i2} + \ldots + e_{i\nu}x^{i\nu} \tag{3.3}$$

We can obtain the syndrome by replacing x by $\alpha^j, j=1,\ldots 2t$, and letting

$$S_j = e(\alpha^j). \tag{3.4}$$

For simplicity of description we define the error magnitude $Y_l = e_{il}$, and the error-location number $X_l = \alpha^{il}$ for $l = 1, \ldots, \nu$. Then Equation (3.4) can be expressed as the following simultaneous equations

$$\begin{aligned}
S_1 &= Y_1X_1 + Y_2X_2 + \ldots + Y_\nu X_\nu \\
S_2 &= Y_1X_1^2 + Y_2X_2^2 + \ldots + Y_\nu X_\nu^2 \\
S_3 &= Y_1X_1^3 + Y_2X_2^3 + \ldots + Y_\nu X_\nu^3 \\
&\vdots \\
S_{2t} &= Y_1X_1^{2t} + Y_2X_2^{2t} + \ldots + Y_\nu X_\nu^{2t}.
\end{aligned} \tag{3.5}$$

The solution of these equations is unique and gives the error magnitudes and their location. It is difficult to solve this set of nonlinear equations directly. However we can use the following polynomial.

$$\Lambda(x) = \Lambda_v x^v + \Lambda_{v-1} x^{v-1} + \ldots + \Lambda_1 x + 1 \tag{3.6}$$

This is the error polynomial, which is defined to be the polynomial with zeros at the inverse error locations X_l^{-1} for $l = 1, \ldots, v$. That is

$$\Lambda(x) = (1 - xX_1)(1 - xX_2)\ldots(1 - xX_v) \tag{3.7}$$

By manipulating Equations (3.6) and (3.7), we can get the following matrix

$$\begin{bmatrix} S_1 & S_2 & S_3 & \ldots & S_{v-1} & S_v \\ S_2 & S_3 & S_4 & \ldots & S_v & S_{v+1} \\ S_3 & S_4 & S_5 & \ldots & S_{v-1} & S_{v+2} \\ \ldots & \ldots & \ldots & \ldots & \ldots & \ldots \\ S_v & S_{v+1} & S_{v+2} & \ldots & S_{2v-2} & S_{2v-1} \end{bmatrix} \begin{bmatrix} \Lambda_v \\ \Lambda_{v-1} \\ \Lambda_{v-2} \\ \ldots \\ \Lambda_1 \end{bmatrix} = \begin{bmatrix} -S_{v+1} \\ -S_{v+2} \\ -S_{v+3} \\ \ldots \\ -S_{2v} \end{bmatrix} \tag{3.8}$$

Solving this equation we may obtain the error location polynomials. The error location is given by the zeros of the error location polynomial, which are found using a Chien search [25]; the magnitudes of the errors are given by Forney's algorithm [23].

3.3 Symbol Error Rate Performance of RS Codes

Code words which contain more than t+1 errors will not be corrected. This fact allows us to obtain a performance approximation. When we use BPSK/QPSK with an RS code, the probability of a code word containing i errors can be calculated by the following code word error probability,

$$P(i) = \binom{N}{i} P_e^i (1 - P_e)^{N-i}, \tag{3.9}$$

where $P(i)$ is the code word error probability and N is the number of symbols and P_e is the probability of a symbol error at the input of RS decoder. The probability of symbol error is approximated by taking the mean of the number of erroneous symbols using the above equation and dividing that by the total number of code symbols:

$$Pes = \frac{1}{N}\sum_{i=t+1}^{N} iP(i)$$

$$= \frac{1}{N}\sum_{i=t+1}^{N} i\binom{N}{i}P_e(1-P_e)^{N-i}. \tag{3.10}$$

Furthermore, if the symbols are converted to binary digits, the bit error probability can be written as follows[25 -p.430].

$$Peb = \frac{2^{m-1}}{2^m - 1}Pes \tag{3.11}$$

Figure 3-1 shows the bit error rate performance of BPSK/QPSK with RS codes for m=8, N=255 and t=1~15. As t increases, the performance is improved. The cost of this performance improvement is bandwidth expansion and higher decoder complexity.

Figure 3.2 shows the performance of PSK with RS codes for m=5~8 and a code rate of approximately 0.9. Since m is the number of bits in a symbol and 2^m-1 is the number of symbols in a code word, the complexity of decoders increases with m.

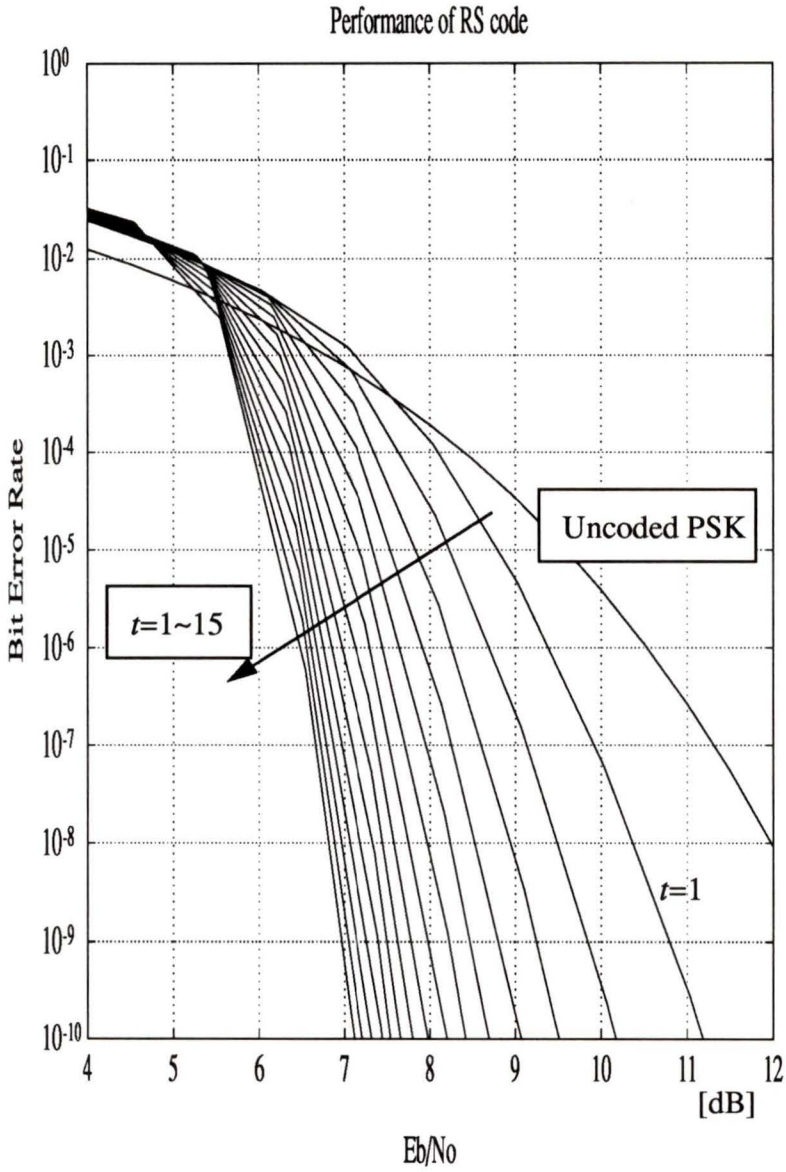

Figure 3.1 The bit error performance of BPSK/QPSK with RS codes with t=1~15, m=8

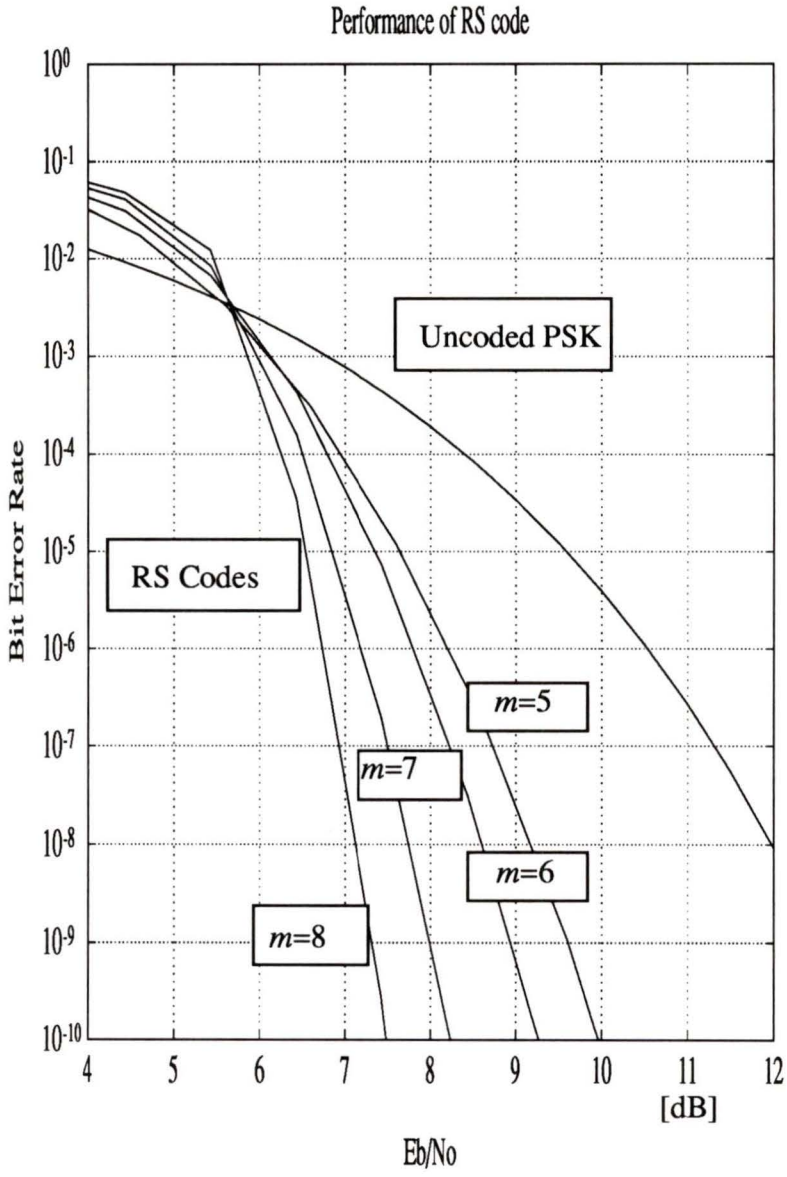

Figure 3.2 The bit error performance of PSK with RS codes with m=8,7,6,5 and a code rate of approximately 90%.

3.4 Erasure and Error Decoding

For efficient decoding of Reed-Solomon codes, we can consider an erasure and error decoding scheme. In this section we will analyze the performance of the erasure and error decoding of an RS Code.

Let us consider an (n,k) RS code with a minimum distance d_{min}. With erasure and error decoding, it is known [23-p.213] that correct decoding can be guaranteed as long as

$$2e + s \le d_{min} - 1, \tag{3.12}$$

where e is the number of code symbol errors in a code word and s is the number of symbol erasures in a code word.

Suppose the error probability of a code symbol is P_e and the erasure probability of a code symbol is P_s. Then the code word error probability is

$$P_w = \sum_{e=0}^{t} \binom{n}{e} \sum_{s=d-2e}^{n-e} \binom{n-e}{s} P_e^e P_s^s (1-P_e-P_s)^{n-e-s} + \sum_{e=t+1}^{n} \binom{n}{e} P_e^e (1-P_e)^{n-e}, \tag{3.13}$$

where $t = \left\lfloor \frac{d-1}{2} \right\rfloor$,

$\lfloor x \rfloor$ is the largest integer smaller than or equal to x.

The symbol error rate P_{sb} can be approximated using P_w as:

$$P_{sb} = \frac{2t+1}{n} p_w. \tag{3.14}$$

And

$$P_b = \frac{2^{k-1}}{2^k - 1} P_{sb} \tag{3.15}$$

Thus, when P_e and P_s are given P_b can be obtained from Equations (3.13) to (3.15).

In Chapter 5 we will discuss how to obtain these probabilities from the super-channel which consists of the channel coding and the Viterbi algorithm.

3.4.1 Performance of Erasure and Error Decoding

In the above discussion we showed the formula for calculating the bit error rate for a RS code. In this section we will find how many symbols should be erased to improve the bit error rate performance. We will find the performance of the RS codes for a given bit error rate for PSK with an erasure probability of P_s. If we define the P_{psk} as the bit error rate of uncoded PSK, we can write the probability of symbol errors at the input of the RS decoder as:

$$P_e = 1 - (1 - P_{psk})^m \tag{3.16}$$

The probability of erasure of a symbol in a code word cannot be defined, since it depends on the method of obtaining erasure information, which is discussed in Chapter 5. For the purpose of knowing how the probability of erasure affects improvement in the bit error rate, we can give the probability of erasure of a symbol in a code word and calculate the performance for an erasure and error decoding scheme. P_s should be measured by an inner coding decoder, *i.e.* Viterbi decoder. For simplicity of analysis, however, we assume the erasures occur randomly only for erroneous symbols with the probability P_s. This means that erasures happen only on the erroneous symbols. Since symbol errors are erased by the inner decoder, the true symbol error probability is given by

$$P^i_{se} = (1 - P_s) \{1 - (1 - P_{psk})^m\} \tag{3.17}$$

where P_s is the probability of erasure of a symbol in a code word. Thus we can calculate the probability of error of a code word from Equations (3.13), (3.14), and (3.15).

Figures 3.3 to 3.7 show the results of calculation of the performance of an erasure and error decoder in the case of t= 1~15, with a moderately high rate (n,k) code $(R \geq 0.9)$. The erasure probabilities are P_s=0.80 to 0.98. These are compared to the performance of a system using uncoded PSK. At a bit error rate (BER) of 10e-5, hard decision decoding of an RS (255,231) code gives a 3 dB coding gain. However, when the bit error rate of the input of the RS decoder is around 10e-2, no coding gain is achieved. This implies that a RS code is not suitable at low E_b/N_0.

However, once we introduce side information for erasures, we can achieve substantial improvement in the system performance.

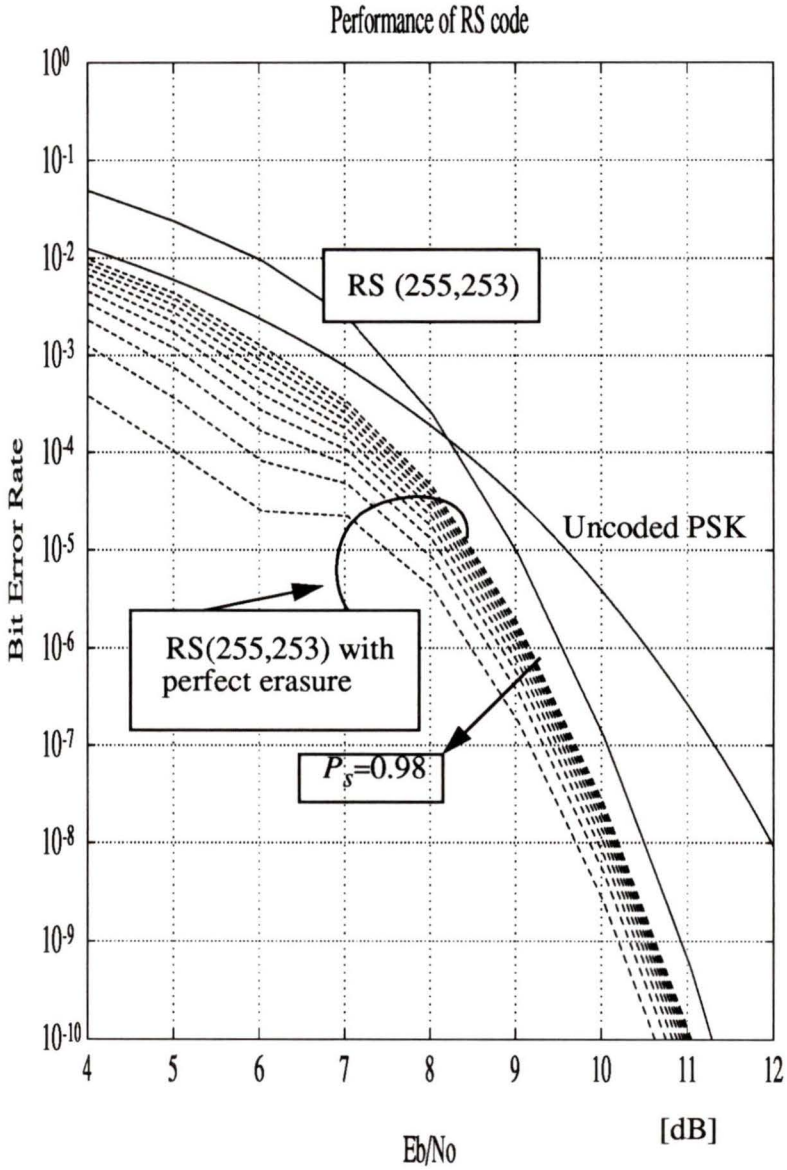

Figure 3.3 The performance of an RS(255,253) erasure and error decoder with P_s=0.8~0.98

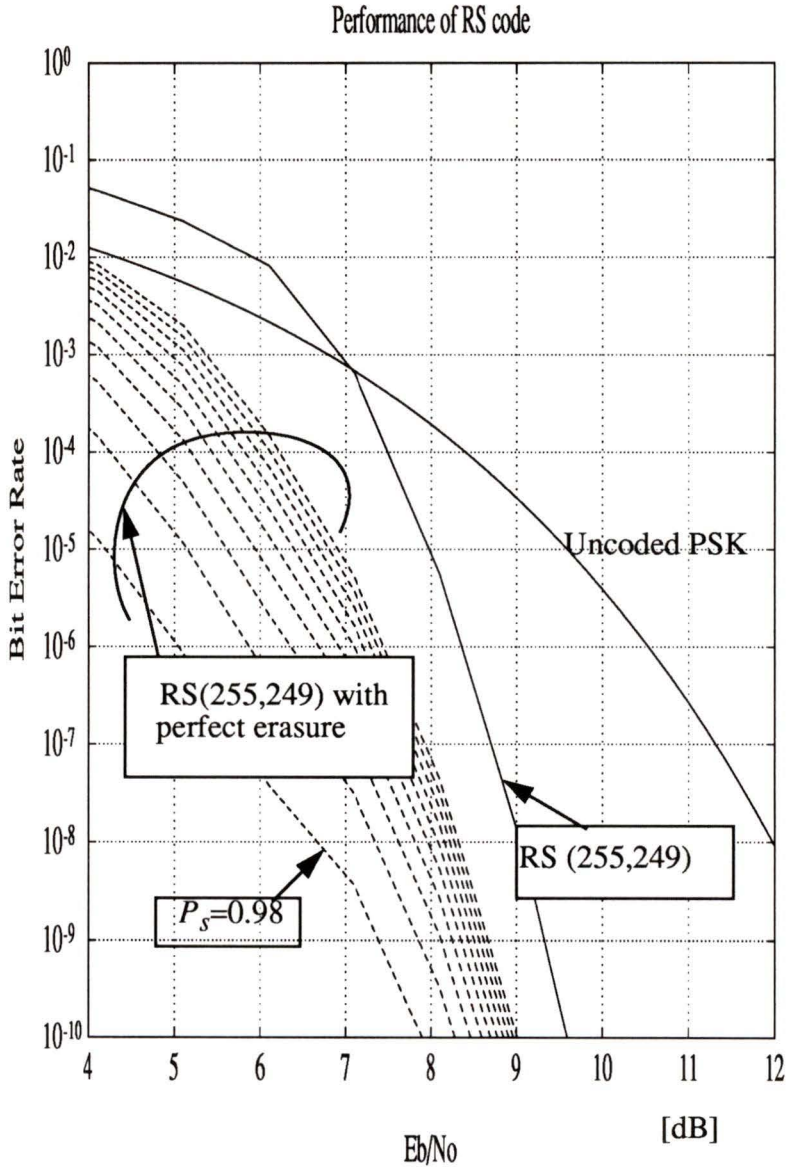

Figure 3.4 The performance of an RS(255,249) erasure and error decoder with P_s=0.8~0.98

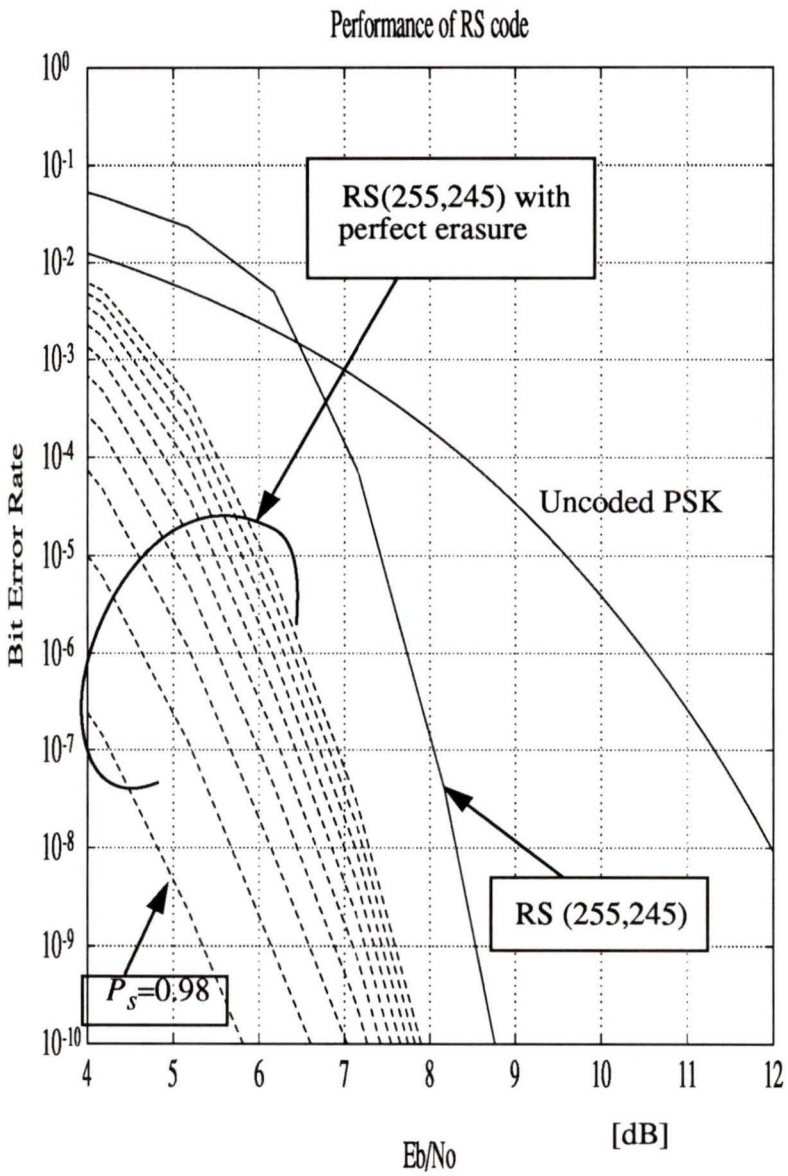

Figure 3.5 The performance of an RS(255,245) erasure and error decoder with P_s=0.8~0.98

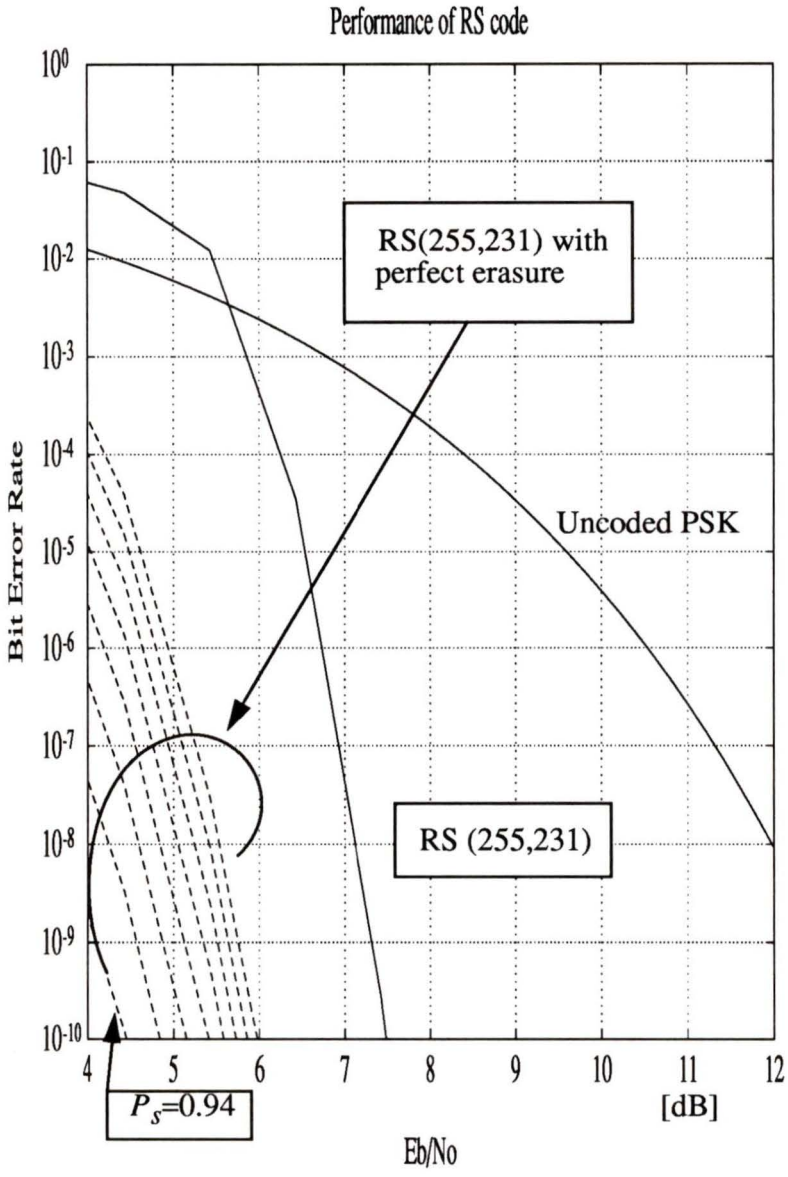

Figure 3.6 The performance of an RS(255,231) erasure and error decoder with P_s=0.8~0.98

3.5 Summary

In this chapter we reviewed the basic characteristics of RS codes, including their representation, decoding algorithm and performance. We also looked into the performance of erasure and error decoding with a given erasure ratio P_s for various t.

These results obtained imply that we can expect further improvements in the bit error rate performance at low E_b/N_0 if erasure information is properly obtained.

Chapter 4

Concatenated TCM-RS Coding System

Trellis coded modulation can provide high coding gain as we have seen in Chapter 2. We can further improve the coding gain of the system by using an RS code as an outer code. The concatenation of TCM with RS codes is analogous to a concatenated coding system using a convolutional code as the inner code and an RS code as the outer code, which was studied by Odenwalder [13]. We can expect comparable improvements in the bit error performance for a concatenated coding system of TCM and an RS code. In this chapter we will examine the coding gain of the concatenated TCM-RS coding system, with a view to its suitability for band-limited and power-limited channel such as mobile and mobile satellite communications.

4.1 System Configuration

Figure 4.1 shows the concatenated coding system that uses TCM and RS codes. The input binary data is coded by an RS encoder into blocks of $2^m - 1$ symbols of m-bits. The output of the RS encoder is fed into a convolutional encoder, which generates an output corresponding to the labels on the trellis diagram. This output is mapped into an 8PSK signal. The additive white Gaussian noise channel and Rayleigh fading channel are considered here. Thus at the receiver, the received signal can be written as

$$\bar{r} = \rho\bar{x} + \bar{n} \tag{4.1}$$

where ρ is the Rayleigh distributed random valuable, which is 1 for the case of the white Gaussian noise channel, and $\bar{n}$ is the additive white Gaussian noise. After the received signal is detected by a matched filter, it is decoded by the Viterbi decoder, and then formed into m-bit symbols and further decoded using a Reed Solomon decoder.

For simplicity, we assume infinite interleaving of the output of the Viterbi decoder. This can be assumed if enough depth of interleaving is used. Using this assumption, we can calculate the performance of the concatenated coding system with various RS codes.

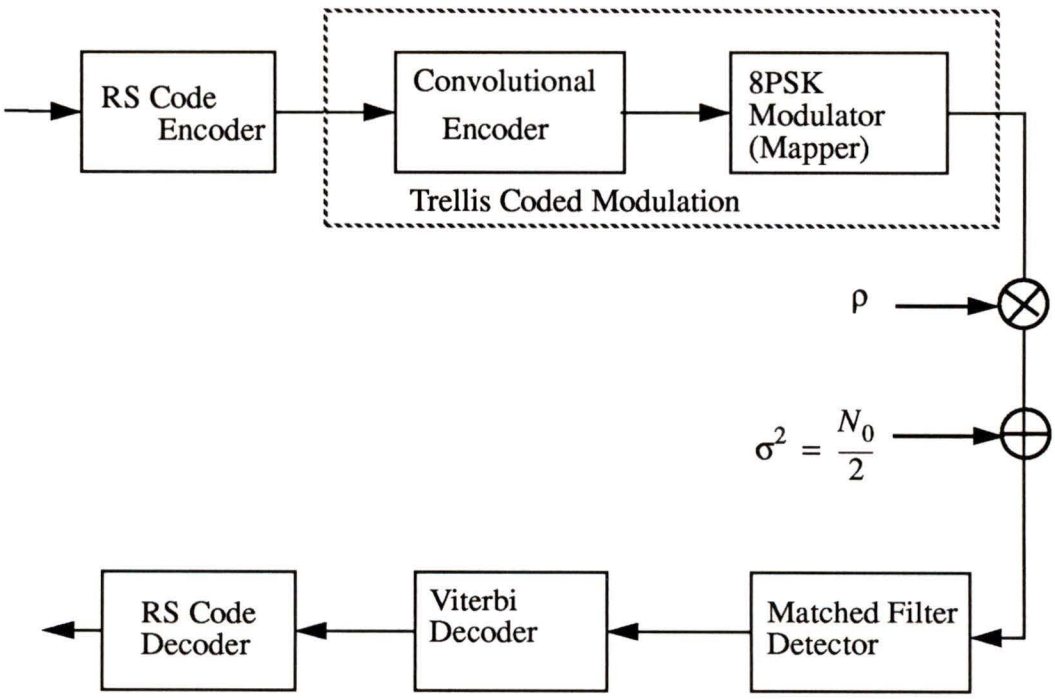

Figure 4.1 The concatenated coding system using TCM and RS codes

4.2 Performance of a Concatenated Coding System with RS Codes

The performance of the concatenated coding system is compared with various values of m and t. One comparison is done by computer simulation, another using the theoretical bound of the performance of TCM.

4.2.1 Theoretical Bound Derivation

We begin by discussing the performance of the concatenated code system and deriving the upper bound of bit error rate for the concatenated TC-8PSK with RS codes. The upper bound of the bit error rate for the TC-8PSK is given in Equation (2.20) and is repeated here:

$$P_{TCM}\left(\frac{E_s}{N_0}\right) = \frac{1}{2}\frac{\partial}{\partial I}T(D,I)\Big|_{I=1,\,D=exp(-Es/4N0)} \tag{4.2}$$

and

$$P_{TCM}\left(\frac{E_s}{N_0}\right) = P_{TCM}\left(\frac{2E_b}{N_0}\right) \tag{4.3}$$

Then the symbol error rate at the input of the RS decoder is defined as:

$$P_e = 1 - \{1 - P_{TCM}\left(R\frac{2E_b}{N_0}\right)\}^m, \tag{4.4}$$

where R is the code rate of an RS code. Since the symbol error rate of the input symbols of an RS code is given by Equation (4.4) then the bit error rate may be written as:

$$P_{bit} = \frac{2^{m-1}}{2^m - 1}\frac{1}{N}\sum_{i=t+1}^{N} i\binom{N}{i}P_e^i(1-P_e)^{N-i} \tag{4.5}$$

Upper bounds of bit error performance are shown in Figure 4.2 for 1 to 15 correctable errors and m=8.

At a bit error rate of 10e-4, concatenating the coding systems with RS codes result in improvement in the equivalent E_b/N_0 of 0.1 dB to 1.0 dB as compared to TC-8PSK without an RS code. The coding gain is obtained at the cost of bandwidth expansion.

The code rate and coding gain for various RS codes are shown in Table 4.1.

(n,k,t) code	Rate	Gain of E/N at 10e-4
(255,253,1)	0.992157	0.05dB
(255,251,2)	0.984314	0.30dB
(255,249,3)	0.976471	0.44dB
(255,247,4)	0.968627	0.51dB
(255,245,5)	0.960784	0.55dB
(255,243,6)	0.952941	0.57dB
(255,241,7)	0.945098	0.59dB
(255,239,8)	0.937255	0.60dB
(255,237,9)	0.929412	0.60dB
(255,235,10)	0.921569	0.70dB
(255,233,11)	0.913725	0.76dB
(255,231,12)	0.905882	0.81dB
(255,229,13)	0.898039	0.83dB
(255,227,14)	0.890196	0.84dB
(255,225,15)	0.882352	0.85dB

Table 4.1. Code rate and coding gain of RS codes

It can be seen from Table 4.1 that the rate of the improvement of E_b/N_0 becomes less around t=12. Thus, the case of t=12 is a good choice for considering the rate of bandwidth expansion. Of course the allowance for the system bandwidth expansion totally depends on the system. Therefore, we choose t=12 as one of efficient concatenated coding systems and the bandwidth expansion is to be 0.90 for our interests.

Next we are interested in the different size of the blocks of the RS codes. In practice the issue of realization is very important, that is, the complexity and cost of a decoder is one of factors we have to consider when designing a coding system. As the

size of the codes become larger, the more difficult and expensive to realize. In this sense it would be better to realize the same performance with a shorter code. For comparison we use the fixed code rate R=0.90 and considered codes with, m=5,6,7,8 as in Table 4.2.

(n,k,t)- m	code rate	improvement
(255,231,12) -8	0.9059	0.95dB
(127,115,6) - 7	0.9055	0.7dB
(63,57,3) -6	0.9047	0.5dB
(31,27,2) -5	0.8709	0.3dB

Table 4.2. Coding Gain for RS codes

The above approximations, however, are not valid if E_b/N_0 is low, as may be the case for mobile communication channels. but a good approximation of the performance can be obtained through simulation. This is because we can simulate the error distribution of the inner decoder. The errors are subject to bursts and RS codes are good for dealing with burst errors. By using simulation results we can calculate the symbol errors for the input symbols of an RS code. The final bit error rate is calculated using Equation (4.5).

The results of the simulation are shown in Figure 4.4 and Figure 4.5. Figure 4.4 shows the bit error rate for the performance of the concatenated coding system of TCM and RS codes with t=1 to 15. Figure 4.5 shows the performance of the concatenated coding system with m=5,6,7,8 and a code rate of approximately 0.90. These figures can be compared to Figure 4.2 and Figure 4.3, which show the approximation of the bit error rate performance of the concatenated coding system. The difference in E_b/N_0 is 0.5 dB at 10e-4 and 1.0 dB at 10e-1. These differences exist mainly because the Viterbi decoder output sequence contains burst decoding errors and the RS code is very efficient at correcting burst errors. The Viterbi decoder has a high potential to correct errors with a maximum

likelihood rules. Theoretically, one symbol could be correctly received by observing the path metric over an infinite time period. In practice, however, we have to use the truncated Viterbi algorithm. Thus, the output of the decoder has errors caused by selecting the wrong paths. Once a wrong path has been selected, the path contains erroneous symbols and it takes time to return to the correct path. This results in burst errors. We assume that ideal symbol-by-symbol interleaving is employed, while in the previous section we assumed infinite bit-by-bit interleaving.

Figure 4.6 shows the performance of the concatenated coding system with m=5,6,7,8 on a Rayleigh fading channel. The simulation data for a Rayleigh fading channel that was shown in Figure 2.11 was used for the bit error rate at the input of the RS decoder. The final bit error rate is calculated using Equation (4.5) as well as the case of AWGN channel. As the channel condition is bad, the improvement in bit error rate can not be obtained by the concatenated TC-8PSK with RS-codes, which is effective in the case of an AWGN channel. This result shows that a TC-8PSK RS coding system requires further improvement to overcome the degradation of performance when it operates in the case of a Rayleigh fading channel.

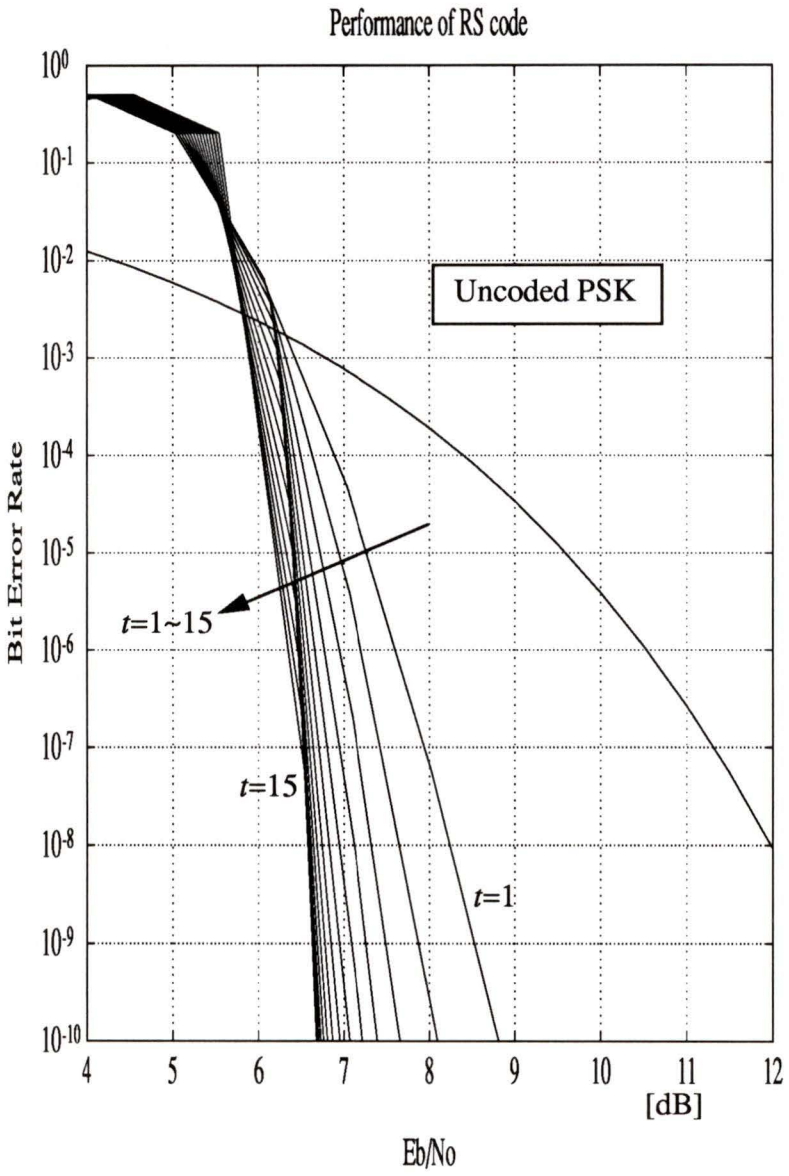

Figure 4.2 The upper bound of bit error performance of TC-8PSK concatenated with RS codes with various t, m=8.

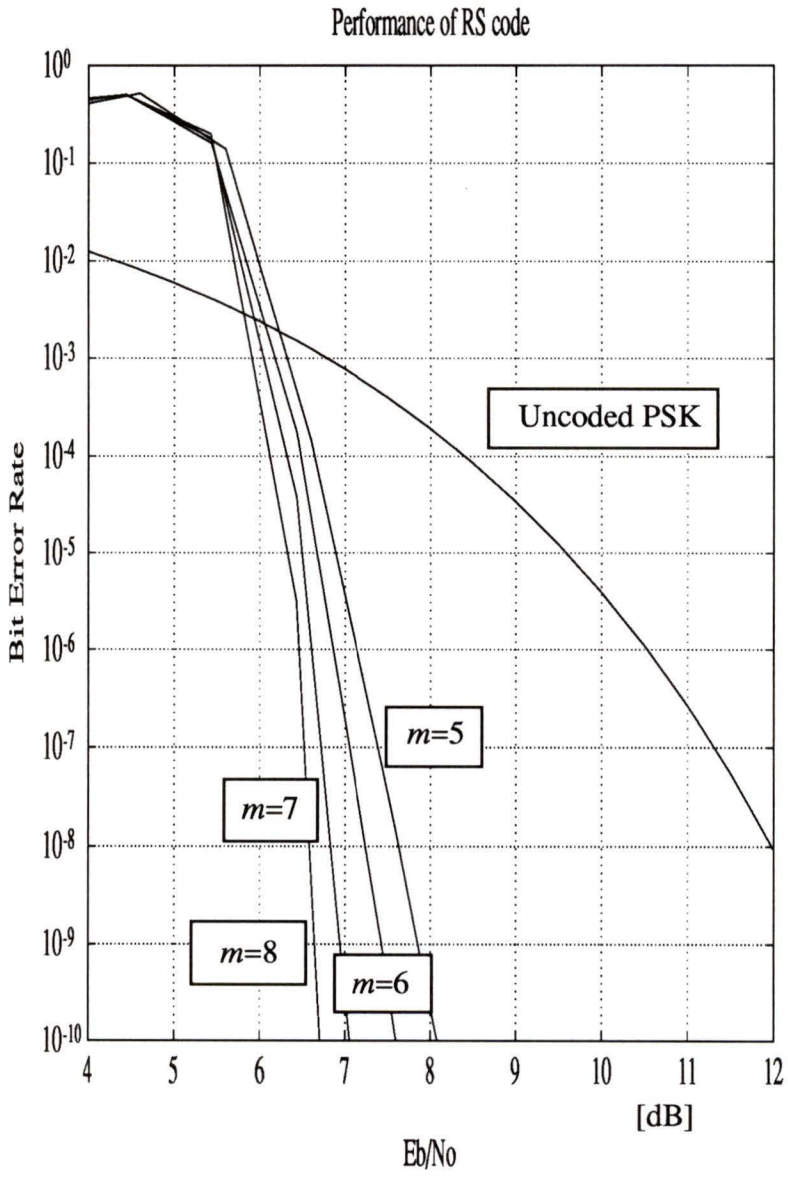

Figure 4.3 The upper bound of bit error performance of TC-8PSK with RS codes with m=5,6,7,8 for a code rate about 0.9

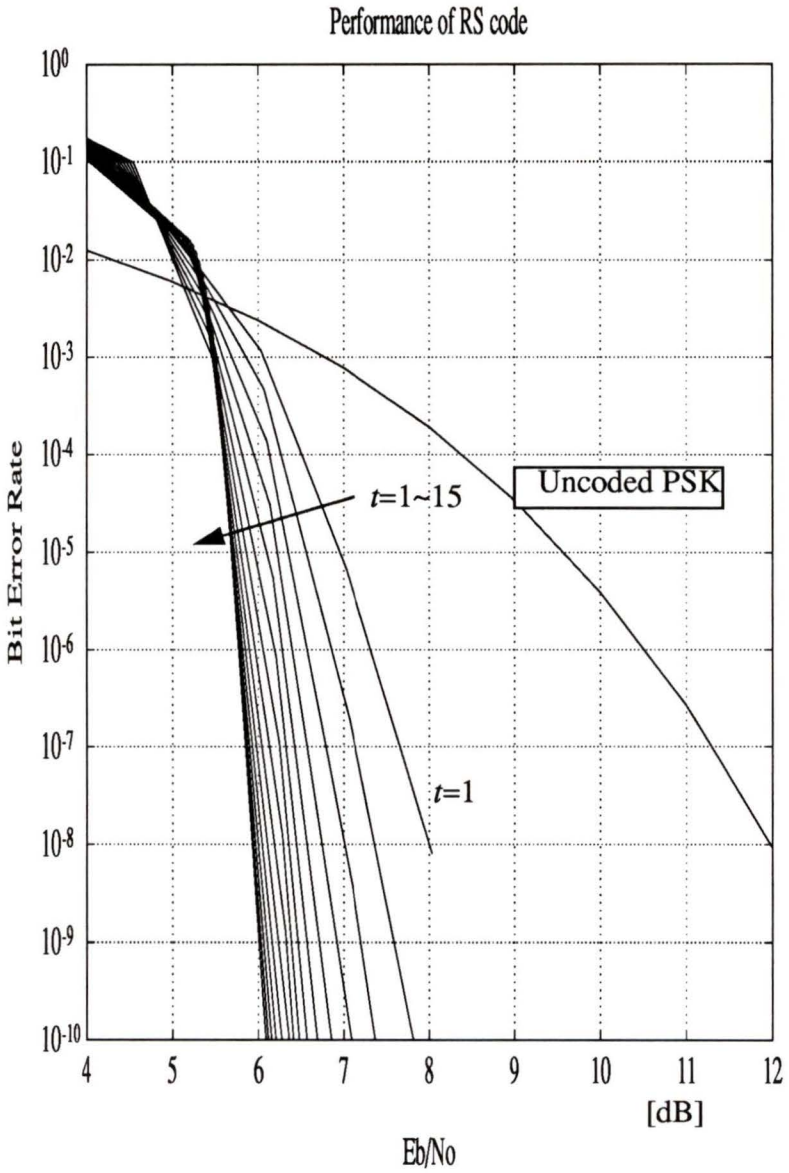

Figure 4.4 The bit error performance of TC-8PSK with RS codes calculated by the simulation of TC-8PSK and using the formula for RS with t=1~15 and m=8

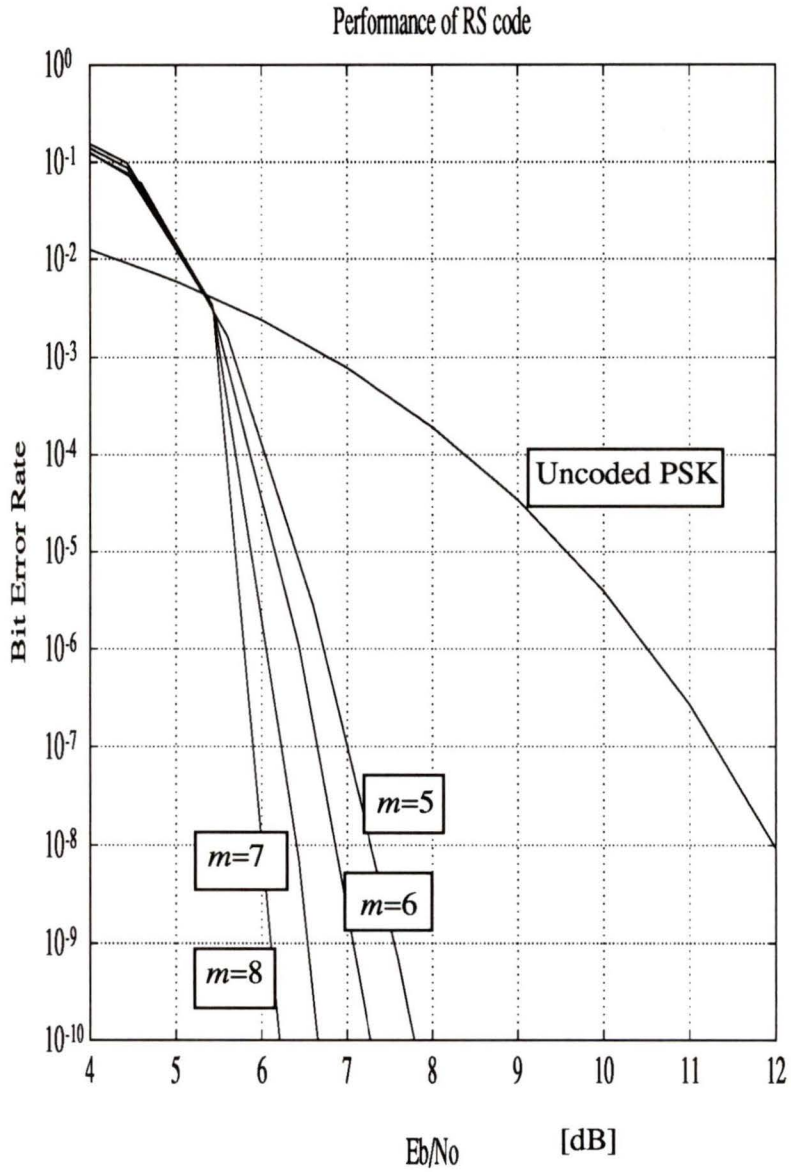

Figure 4.5 The bit error performance of the concatenated system with TC-8PSK and RS codes with m=5,6,7,8 and Rate 90%

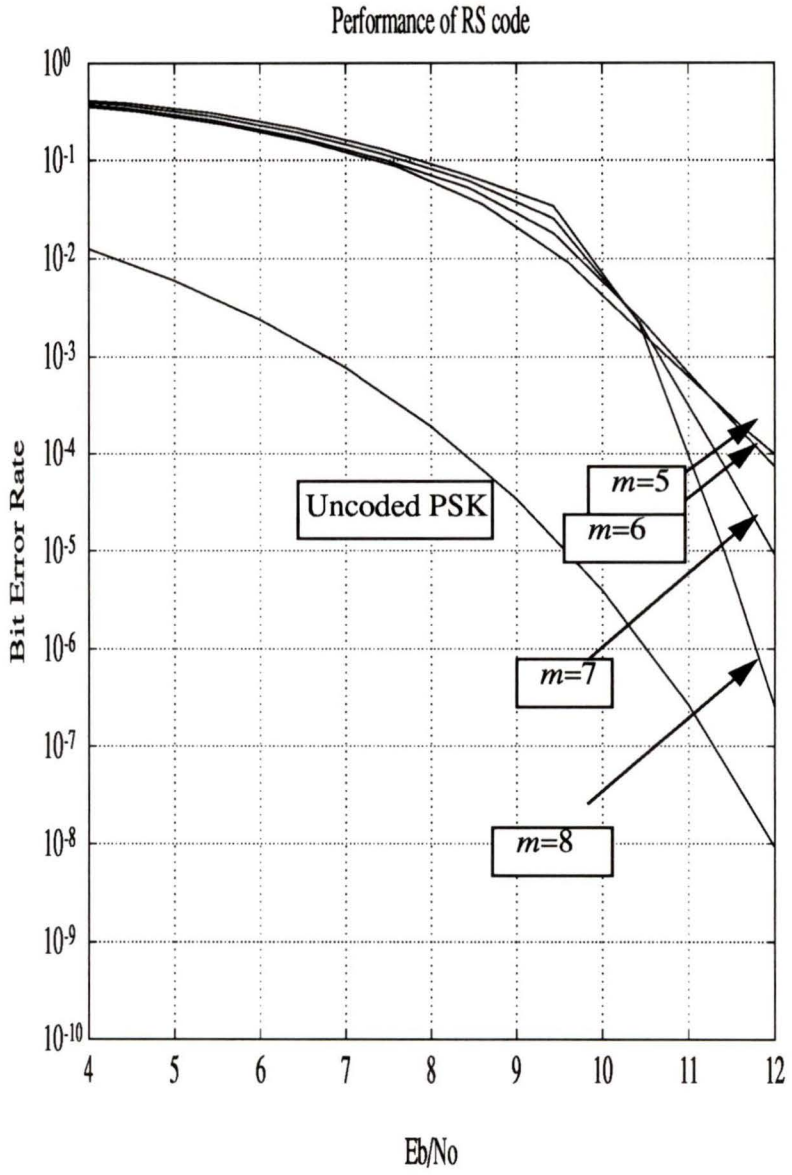

Figure 4.6 The bit error performance of the concatenated coding system with TC-8PSK with RS codes with m=5,6,7,8 and rate 90% on a Rayleigh fading channel

4.3 Summary

In this chapter we presented a concatenated coding system with TC-8PSK and RS codes. The performance of the system was determined using two methods: the upper bound, and by computer simulation. Because of burst errors caused by the Viterbi decoder and the Reed-Solomon decoder's ability to correct burst errors, the bit error rate performance of the two methods is different when E_b/N_0 is low.

The simulation results showed the improvement in the BER for the concatenated coding system, which is 0.80 dB at a BER=10e-4 when t=12 and m=8, as compared to a TCM system without a concatenated RS code.

Chapter 5

Performance of the Concatenated Coding System with a Modified Viterbi Decoder

In Chapter 3 we showed the bit error rate performance RS codes can be improved by using erasure and error decoding. In the same manner, we can expect further improvement in the performance of TCM concatenated with RS codes by introducing erasure and error decoding. In order to realize this erasure and error decoding of RS codes, it is necessary to extract the reliability information with respect to the input symbols to the RS decoder. In practice, an RS decoder uses a hard decision rule. In this thesis, we are also assuming a hard decision RS decoder. For erasure and error decoding, the reliability for an RS code is based on erasure declaration. In a concatenated coding system, an inner decoder could forward this erasure declaration information to an outer RS code. A modified Viterbi algorithm with erasure information has been reported [9][11][6].

Hagenauer [10] described a Viterbi algorithm with soft-decision outputs and showed the application to the concatenated coding system with two sets of convolutional codes. We show the application to the erasure declaration of the Viterbi decoder by using the reliability function with a truncated Viterbi decoder that he defined.

Furthermore, we propose a new modified Viterbi decoder. The performance of the system with the modified Viterbi decoder is discussed.

5.1 A Modified Viterbi Decoder with Erasure Detection

In practice, the cumulative Euclidean distance is often used as a path metric for simplicity. We have also used this path metric, although it is not ideal for channels other than an AWGN channel. The soft-output Viterbi algorithm [10] uses reliability information in the following manner.

Assume that the Viterbi decoder makes a final decision with delay Δ, which is large enough so that all 2^{v} survivor paths have been merged with sufficiently high probability. The state S_k is chosen by selecting the best maximum likelihood metric, which for the AWGN channel is

$$M_m = \frac{Es}{N_0} \sum_{j=k-\Delta}^{k} (\bar{y}_j - \bar{x}_j^{(m)})^2 \text{ ,m=1,2....,} \tag{5.6}$$

where x_j^{m} is the label of the trellis transition of the m-th path. The probability of the m-th path may then be written in the following form:

$$\text{Prob}\{\text{path m}\} \cong exp\,(-Mm)\,, \tag{5.7}$$

and the probability of selecting the wrong survivor's path P_{sk} may be written as

$$p_{sk} = \frac{e^{-M2}}{e^{-M1} + e^{-M2}} = \frac{1}{1 + e^{M2-M1}} = \frac{1}{1 + e^{\Delta}}. \tag{5.8}$$

Hagenauer used this probability to get the soft output of the convolutional decoder. For a concatenated coding system with RS codes, we may use the above probability directly to get the erasure declaration, especially for a truncated Viterbi decoder.

We can apply this probability function to declare the erasure for symbols in the following manner. We use the Viterbi decoder described in Chapter 2 with a decision depth of 15, which is 5 times the constraint length. Using this truncated Viterbi decoder with a window of width L window where L is the decision depth, we can investigate the perfor-

mance of the system. In the last stage of a trellis diagram of this window with 8 states, each state has a survivor path 1 which has the minimum metric $M1$. We also select the second path 2, which has the next smallest path metric $M2$. The difference between the metrics of the two paths is Δ. When Δ is smaller than a given threshold, we can declare erasures at the positions where the symbols of the paths 1 and 2 differ, as shown in Figure 5.1.

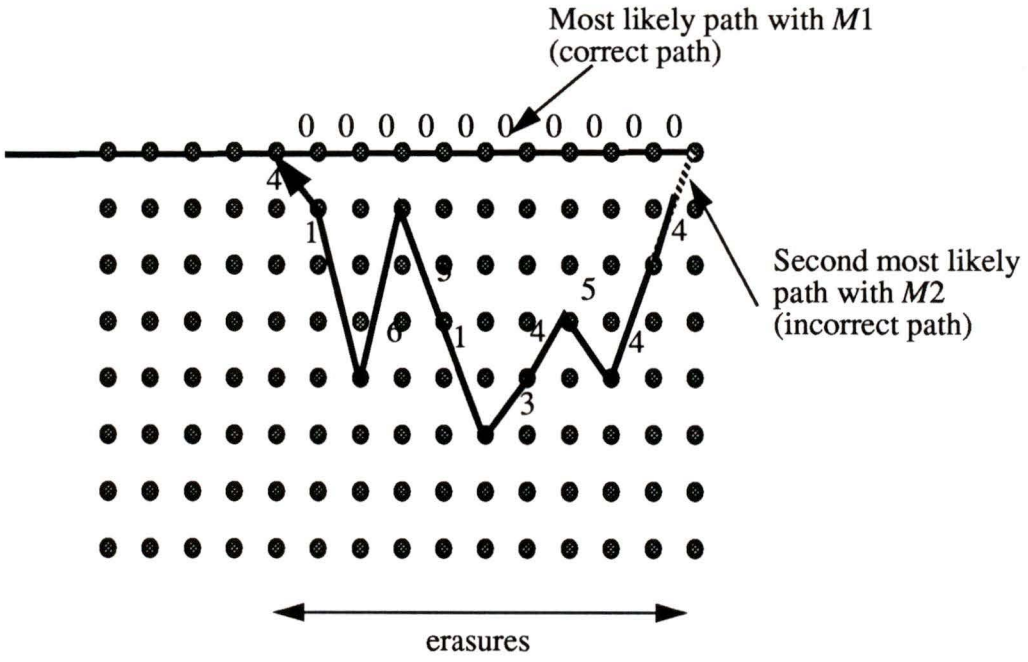

Figure 5.1 Erasure declaration of the path metric competition

This is consistent with the works of Deng [9] and Schaub [6]. They assumed that the two paths are merged in a trace back process. This requires an infinite decision depth

in the Viterbi decoder, and also that the merging paths at the last stage of the window are compared to each other.

Since we are interested in the truncated Viterbi decoder, we apply the above probability function to declare the erasure for the truncated Viterbi decoder and we compare the path metric at just one stage before they will merge to a stage. This is equivalent to saying that we compare all the metrics of the survivor paths and choose the two closest paths. The erasure declaration process is the same as mentioned before.

Figure 5.2 shows the algorithm used by a modified Viterbi decoder. The modification requires additional trace back memory and erasure flag memory.

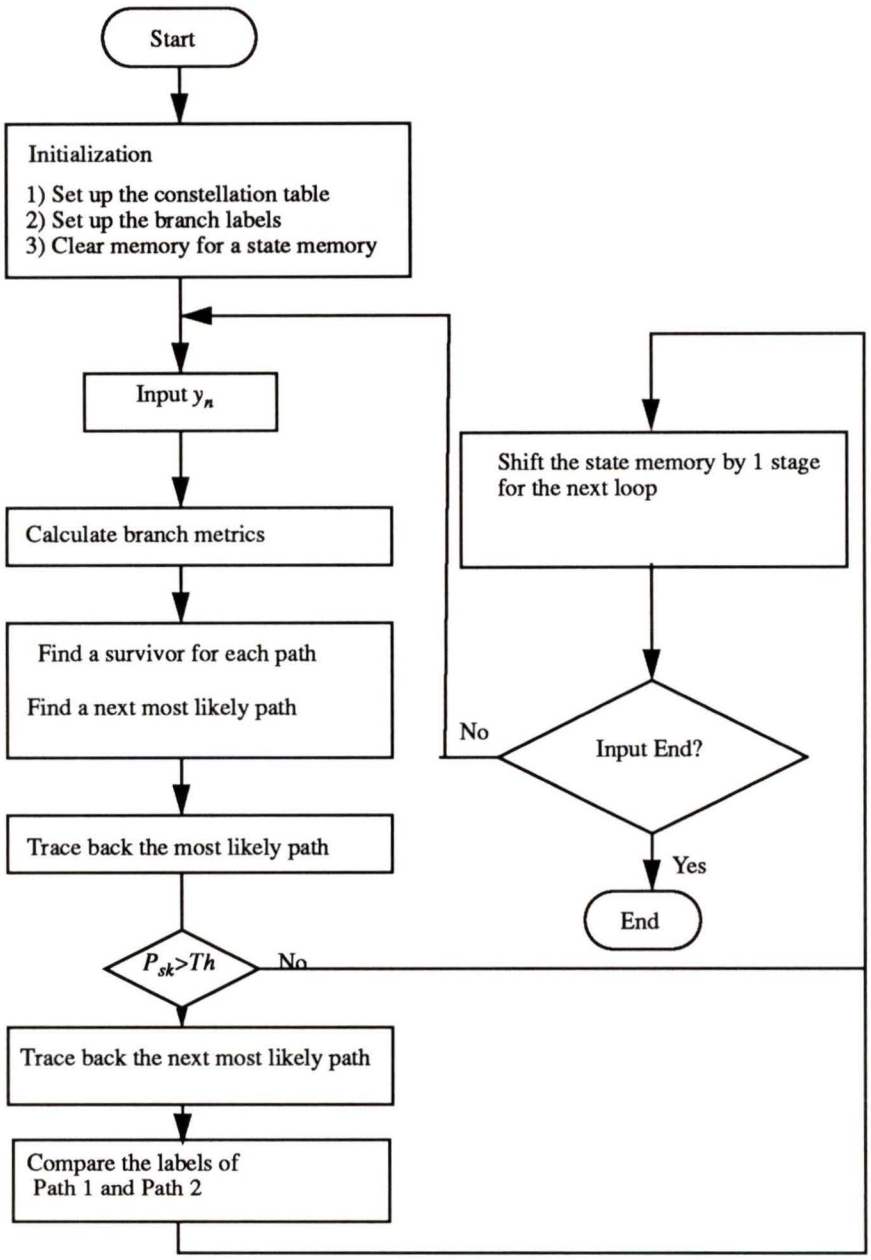

Figure 5.2 A modified erasure declaring Viterbi decoder

Figure 5.3 shows the performance improvement of the system using the above Viterbi decoder. As we decrease the threshold value from 0.5 to 0, we get better overall performance improvement. In particular we notice that we get an improvement in the bit error rate performance at a low E_b/N_0. It can be said that the erasure declaration Viterbi decoder does work at a low E_b/N_0. The improvement trend deteriorates at some point.

Figure 5.4 shows the improvement trends for various thresholds. The optimum threshold can be selected so that the BER is minimized. This threshold depends on E_b/N_0, but we are interested in the performance at low E_b/N_0, so we can select the threshold for a low E_b/N_0.

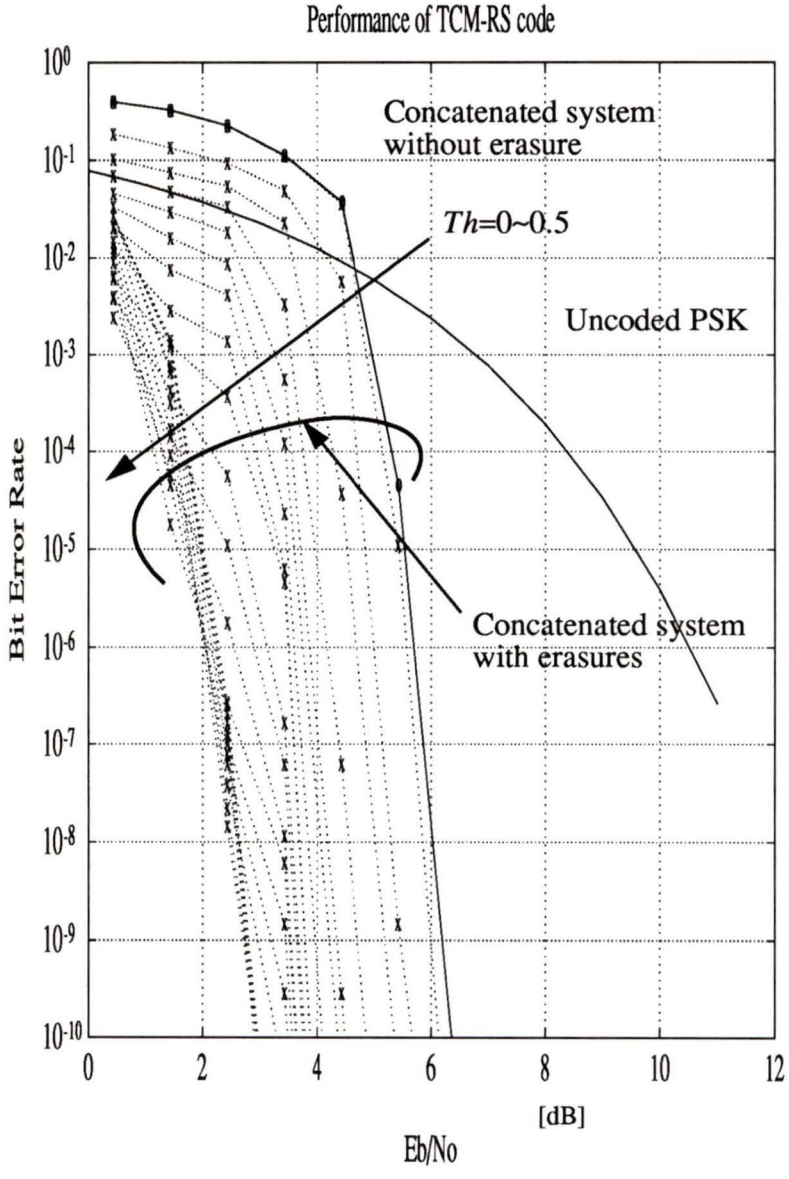

Figure 5.3 The performance of concatenated TC-8PSK with RS (255,231) with a modified Viterbi decoder; Scheme I

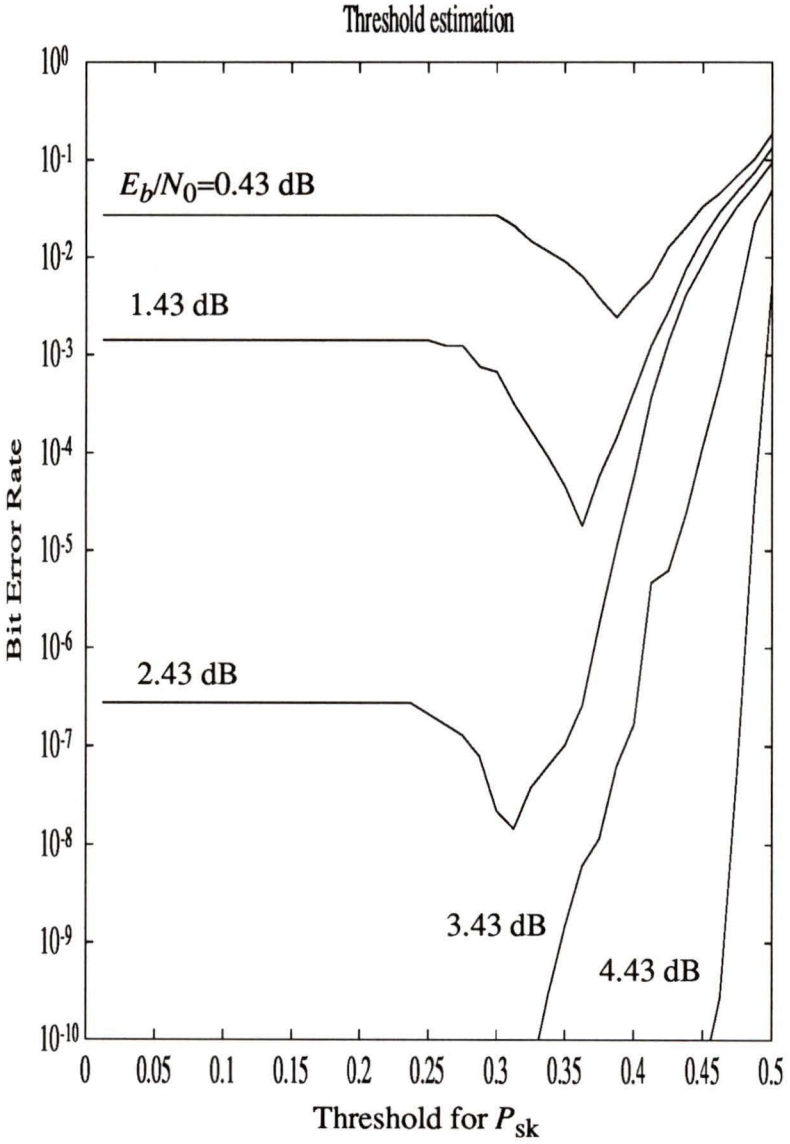

Figure 5.4 The optimum threshold for Scheme I

5.2 A New Scheme of Erasure Declaration for a Modified Viterbi Decoder

The truncated Viterbi decoder chooses the most likely symbol using the selected path with the minimum metric for a decision depth 15 symbol intervals. We can not decide the symbol at the window period because the best path would be different from one window to another. The same thing can be said for erasure declaration. For erasure declaration, as for scheme I, we search two paths whose metrics are close by Δ, find positions with different labels on each path, and erase the corresponding symbols. But in this process we notice the metric is to be used for selecting the path and deciding the first symbol of a trellis window. As for Scheme I, we erase symbols which are in the middle of a window. This may result in incorrect erasures. In this sense, Scheme I is not optimal in terms of the erasure information; we therefore propose a new scheme (Scheme II), as described below.

The new method of erasure declaration is based on averaging the reliability information within a window period. We observe L stages in a window, each stage having a most likely path with metric $M1$ and a second most likely path with metric $M2$. At time $t=k$ we determine the probability of selecting the wrong path P_{sk}. For Scheme I, we traced back the two paths to find the positions where the trellis labels were different when P_{sk} is greater than a certain threshold. However, in Scheme II, we observe L stages and take the average of the probabilities of selecting the wrong path. Suppose that at k=15 we have the most likely and the second most likely paths with $P_{sk}[k]$. We check $x_n[k]$ of path 1 and $x_n[k]$ of path 2; if these are different we claim the probability of selecting wrong symbol $x_n[k]$ is $P_{sk}[k]$, otherwise we claim the probability is 0. One stage earlier we determined $P_{sk}[k-1]$ and $x_n[k-1]$ in a similar manner. In this way, we obtain fifteen probabilities of selecting the wrong symbol $P_{sk}[k]$, given that the symbol x_n was transmit-

ted, since x_n is in the window for 15 T_s.

In other words, one symbol has erasure information for L symbols. We can average those and obtain the averaged probability of selecting the wrong path:

$$P_{k=L}\{erase\} = \sum_{k=1}^{L}\left[\frac{1}{1+exp(\Delta_k)}\right]\cdot\Phi_k \tag{5.9}$$

where Φ_k is 1 when the decoded symbols of the most likely and the second most likely paths differ, and zero otherwise.

These L erasure information which is concerned to one symbol of $x_n[k]$ are averaged and compared to a certain threshold when $x_n[k]$ is decoded as the output of the Viterbi decoder.

By using Scheme II, we can simulate the performance of the concatenated coding system with erasure and error decoding. Figure 5. 5 shows the performance of Scheme II. Figure 5.6 shows the performance versus the threshold of the probability. Compared to Scheme I, we have an improvement in the performance, particularly at low E_b/N_0.

We can further simulate the performance of Scheme II in a Rayleigh fading channel. Figure 5.7 shows the performance of concatenated TC-8PSK with RS (255,231) using the Scheme II Viterbi decoder. The threshold of the probability of selecting the wrong path is chosen to be Th=0.25, which gives comparatively good error performance results. Figure 5.8 shows the optimum threshold for P_{sk}. For E_b/N_0 =0.43 dB, the optimum threshold is around 0.2. As E_b/N_0 decreases, the optimum threshold decreases. However, we can select Th= 0.25 because of our interest in the low E_b/N_0 case.

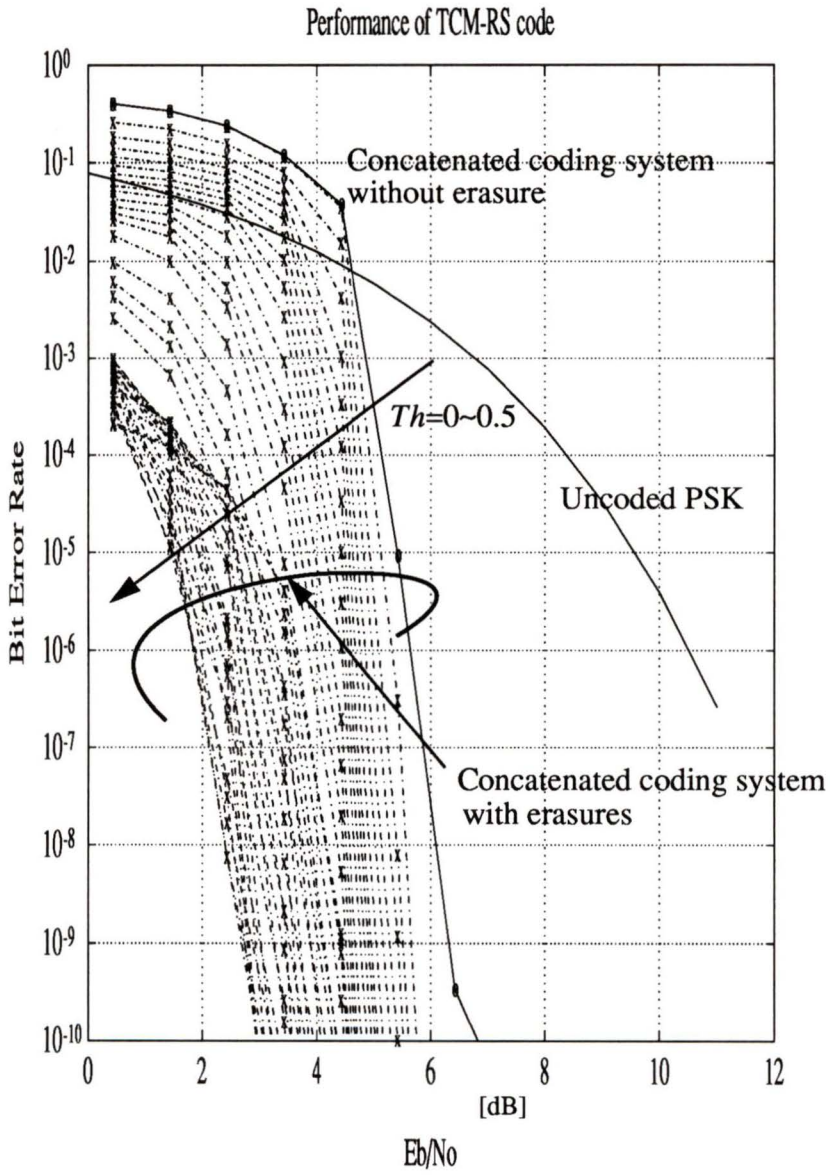

Figure 5.5 The performance of concatenated TC-8PSK with RS (255,231) with a modified Viterbi decoder; Scheme II

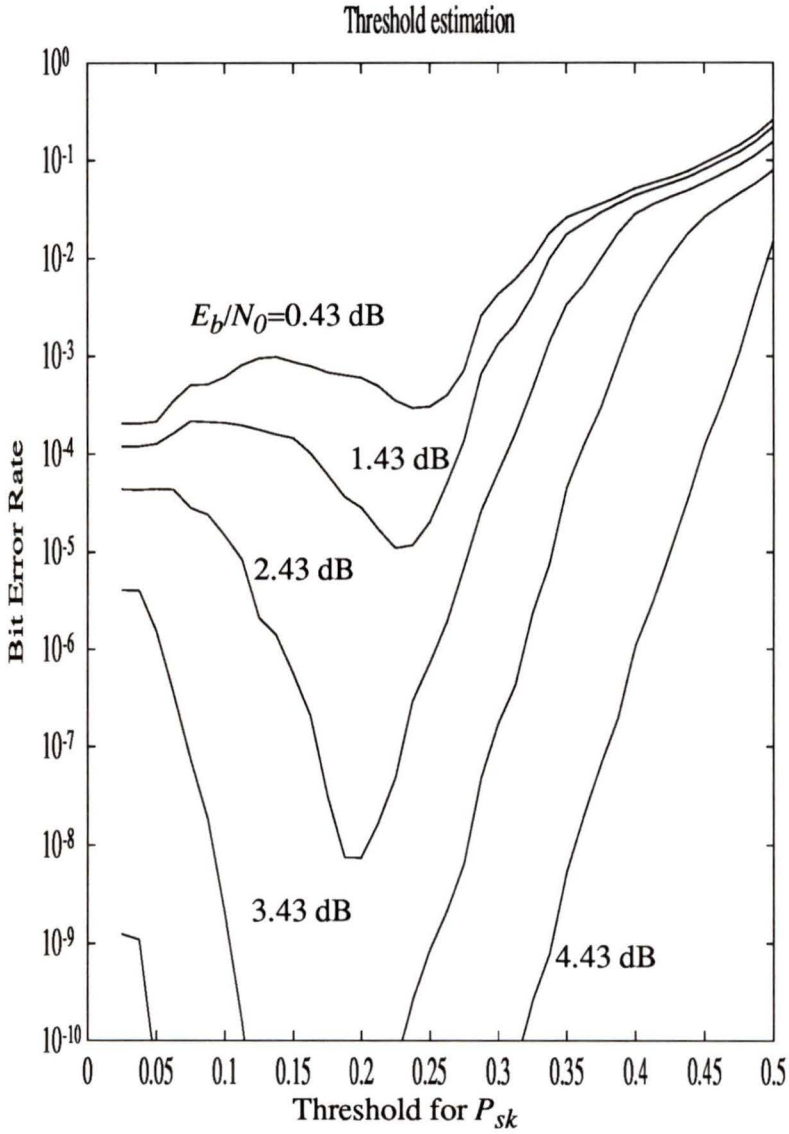

Figure 5.6 The optimum threshold for a new modified Viterbi decoder (Scheme II)

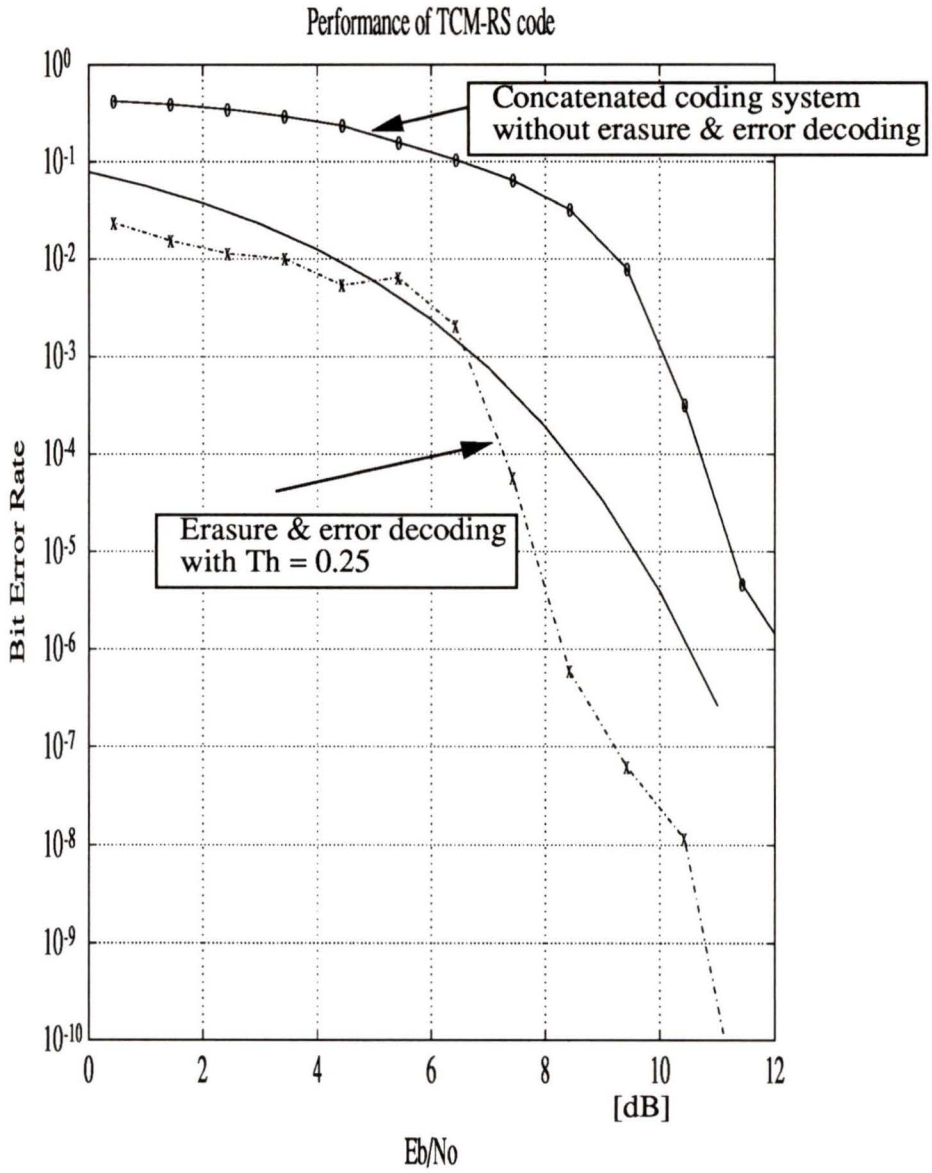

Figure 5.7 The performance of concatenated TC-8PSK with RS(255,231) with Scheme II Viterbi decoder in a Rayleigh fading channel

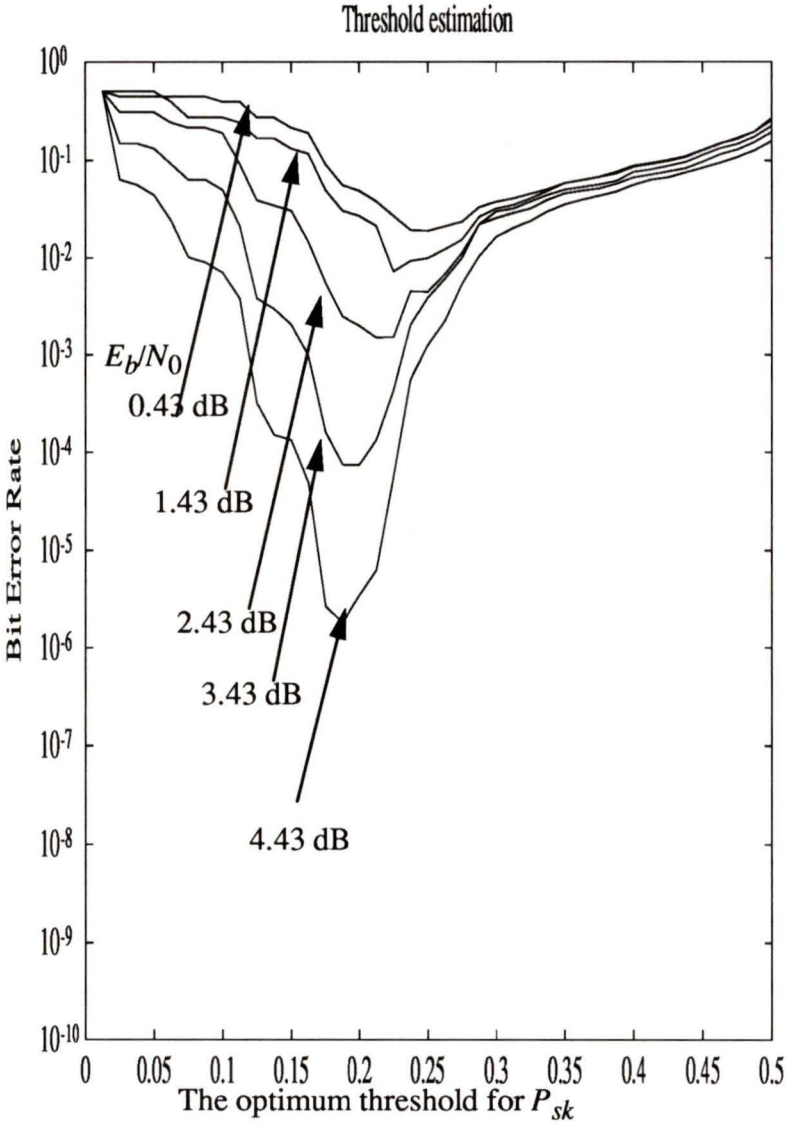

Figure 5.8 The optimum threshold for a new modified Viterbi decoder (Scheme II) in a Rayleigh fading channel

5.3 Summary

We have shown a concatenated coding system with an RS code using a modified Viterbi decoder. We applied the probability of selecting the wrong paths defined by Hagenauer as the value for declaring erasures of the truncated Viterbi decoder. We confirmed that erasure and error decoding with a modified Viterbi decoder offers improved bit error rate performance, particularly at low E_b/N_0. Furthermore, we proposed Scheme II for a new modified Viterbi decoder and confirmed the improvement in performance.

Chapter 6

Conclusions and Future Research

6.1 Summary of the Thesis

The performance of TCM was presented by theory and computer simulations. TC-8PSK achieved a 3.6 dB coding gain asymptotically and a 2.0 dB coding gain at BER =10e-4 without any bandwidth expansion. We concatenated TC-8PSK with a Reed Solomon code and achieved a further improvement in performance of 0.9 dB for m=8 and t=12, but at the cost of an 11% expansion in bandwidth.

We also showed the erasure and error decoding performance of Reed-Solomon decoding. When the erasure information is forwarded to a decoder, the performance of the system was improved. We applied this erasure of errors to the concatenated coding system to realize an additional improvement in the bit error rate performance of the overall system.

By modifying the Viterbi decoder we extracted erasure information. We realized the truncated Viterbi decoder by computer simulation and showed that the erasure information could be used to improve the system performance, even at low values of E_b/N_0. In addition, we proposed a new modified Viterbi decoder which averaged the erasure information over a window.

6.2 Suggestions for Future work

In this thesis, we mainly discussed TC-8PSK in a concatenated system operating over AWGN channel and a Rayleigh fading channel. The following works may be considered in the future:

1. generalization of the performance for the concatenated coding system of TCM and block codes;
2. analysis of the system performance in a correlated fading channel;
3. simplification of the modified Viterbi decoder for LSI implementation.

Bibliography

[1] G. Ungerboeck, "Channel coding with multilevel phase signal," *IEEE Trans. Information Theory*, vol. IT-28, pp. 55-67, Jan. 1982.

[2] G. Ungerboeck, "Trellis-Coded Modulation with Redundant Signal Sets - Part I: Introduction," *IEEE Communications Magazine*, vol. 25, no. 2, pp. 5-11, Feb. 1987.

[3] G. Ungerboeck, "Trellis-Coded Modulation with Redundant Signal Sets - Part II: State of the Art," *IEEE Communications Magazine*, vol. 25, no. 2, pp. 12-22, Feb. 1987.

[4] G.D.Forney, Jr., *Concatenated Codes*, MIT Press, Cambridge, MA 1966.

[5] D. Divsalar and M.K. Simon, "Trellis Coded Modulation for 4800-9600 bits/s Transmission over a Fading Mobile Satellite Channel," *IEEE Journal on Selected Areas in Communications*, vol. SAC-5, no. 2, pp. 162-174, Feb. 1987.

[6] T. Schaub and J. W. Modestino, "An erasure declaring Viterbi decoder and its applications to concatenated coding systems," *IEEE Int. Conf. Commun. Conf. Rec.*, Toronto, Canada, June 1986, pp. 1612-1616.

[7] D. Divsalar and M. K. Simon, "The design of trellis coded MPSK for fading channel: performance criteria," *IEEE Trans. Commun.*, vol. 36, pp. 1004-1012, 1988.

[8] R.G.McKay, et.al. "Error Bounds for Trellis-Coded MPSK on a Fading Mobile Satellite Channel," *IEEE Trans. Commun.*,vol. 39, No. 12.,Dec. 1991.

[9] Deng, R.H. and Costello, D.J., Jr.,"High rate concatenated coding systems using bandwidth efficient trellis inner codes," *IEEE Trans. Commun.*, vol. COM-37, no.5, May 1989, pp. 420-427.

[10] Hagenauer, J. and Hoher, P.,"A Viterbi algorithm with soft-decision output and its applications," *IEEE GLOBECOM*, 1989 pp. 47.1.1-47.1. 7.

[11] H. Yamamoto and K. Itoh, "Viterbi decoding algorithm for convolutional codes with repeat request," *IEEE Trans. Inform. Theory*, vol. IT-26. pp. 540-546, Sept. 1980.

[12] Sadowsky, J.,"A new Method for Viterbi Decoder Simulation Using Importance Sampling," *IEEE Trans. Commun.*, vol. 38., pp 1341-51, Sep. 1990

[13] Odenwalder J. P., "Optimal Decoding of Convolutional Codes," Ph.D. Dissertation, School of Engineering and Applied Science, UCLA, 1970

[14] Heller, J.A. and Jacobs, I.M., "Viterbi Decoding for Satellite and Space Communications," *IEEE Trans.,Commun.Technol.*, COM-19, pp. 835-48,Oct. 1971.

[15] C. Loo, "Measurements and Models of a Mobile-Satellite Link with Applications," *Proc. GLOBECOM '85*, New Orleans, LA., Dec. 2-5, 1985.

[16] C. Loo, "A Statistical Model for a Land Mobile Satellite Link," *IEEE Trans. Vehicular Technology*, vol. VT-34, pp. 122-127, Aug.1985.

[17] C. Loo, E.E. Matt, J.S. Butterworth, and M. Dufour, "Measurements and Modelling of Land-Mobile Satellite Signal Statistics," *1986 Vehicular Technology Conference*, Dallas, Texas, May 20-22, 1986.

[18] P.J. McLane, P.H. Wittke, P.K.M. Ho, and C. Loo, "PSK and DPSK Trellis Codes for Fast Fading, Shadowed Mobile Satellite Communication Channels," *Proc. of IEEE International Conference on Communications*, Seattle, Washington, June 7-10, 1987.

[19] P.J. McLane, P.H. Wittke, P.K.M. Ho, and C. Loo, "PSK and DPSK Trellis Codes for Fast Fading, Shadowed Mobile Satellite Communication Channels," *IEEE Trans. Commun.*, vol. 36, no. 11, Nov. 1988.

[20] A. Papoulis, *Probability, Random Variables, and Stochastic Processes*. New York, McGraw-Hill, 1984.

[21] P. Beckmann, *Probability in Communication Engineering*. New York, Harcourt, Brace and World, pp. 122-123, 1967.

[22] S. Lin and D.J. Costello, Jr., *Error Control Coding: Fundamentals and Applications*. Englewood Cliffs, New Jersey, Prentice-Hall, 1983

[23] G.C. Clark, Jr. and J.B. Cain, *Error-Correction Coding for Digital Communication*. New York, Plenum Press, 1982.

[24] R. E. Blahut, *Theory and Practice of Error Control Codes*. Reading, MA: Addison- Wesley, 1983.

[25] John G. Proakis, *Digital Communications*, 2nd ed. McGraw-Hill Book Company,1989.

[26] B. Sklar, *Digital Communications Fundamentals and Applications*. Prentice-Hall, 1988.

[27] C.W.Therrien, *Decision Estimation And Classification*. John Wiley & Sons,1989.

[28] Lidsey, W.C and Simon, M.K., *Telecommunication Systems Engineering*. Prentice-Hall, Inc., Englewood Cliffs, N.J., 1973.

[29] Korn, I., *Digital Communications*. Van Nostrand Reinhold Company, Inc., New York, 1985.

[30] E. Biglieri *et.al.*, *Introduction to Trellis-Coded Modulation with Applications.* Macmillan Publishing Company, New York.

VITA

Surname: HARADA Given Names: YASUO

Place of Birth: Akashi, Japan Date of Birth: April 8, 1959

Educational Institutions Attended:

Keio University	1978 to 1982
University of Victoria	1991 to 1993

Degrees Awarded:

Bachelor of Engineering	Department of Electrical Engineering, Keio University	1982

Publications:

[1] I. Sasase, Y. Harada, S. Mori, "Bandwidth Efficient Quadrature Overlapped Modulation," *IEEE ICC 82*, June 1982.

[2] I. Sasase, Y. Harada, S. Mori, "The modulation scheme with a superior concentration of the power spectral density: Modified Quadrature Overlapped Raised-Cosine Modulation" *Trans. IECE (IEICE)* vol. J65-B No. 7,July 1982.

[3] I. Sasase, Y. Harada, S. Mori, "Bandwidth Quadrature Overlapped Modulation," *IEEE Trans. Commun.*,vol. COM-32, No.5, May 1984.

[4] T. Nezu, Y. Harada,"PCM Sound Demodulator for Direct Satellite Broadcasting," *National Technical Report*, vol. 30, No. 1, Feb. 1984.

[5] T. Nezu, H. Arita, Y. Harada, "Narrowband Digital Sound Subcarrier for Television Signal" *Institute of Television Eng. of Japan* TEBS 114-6, ED 1011, Dec. 1986.

[6] Y. Harada, T. Nezu, K. Kameda, O. Yamazaki, "MSK Demodulator for Multi-Channel PCM Satellite Broadcasting," *Institute of Television Engineering of Japan* Vol. 11 No. 31, TEBS, Nov. 1987.

Partial Copyright License

I hereby grant the right to lend my thesis to users of the University of Victoria Library, and to make single copies only for such users or in response to a request from the Library of any other university, or similar institution, on its behalf or for one of its users. I further agree that permission for extensive copying of this thesis for scholarly purposes may be granted by me or a member of the University designated by me. It is understood that copying or publication of this thesis for financial gain shall not be allowed without my written permission.

Title of Thesis/Dissertation: **On the Performance of Trellis Coded 8PSK with Reed Solomon Codes**

Author 
(Signature)

Yasuo Harada

April, 19, 1993
(Date)